Physical and chemical properties of non-exhaust particles generated from wear between pavements and tyres

C.A. Alves[1], A.M.P. Vicente[1], A.I. Calvo[2], D. Baumgardner[3], F. Amato[4], X. Querol[4], C. Pio[1], M. Gustafsson[5]

[1]Centre for Environmental and Marine Studies, Department of Environment, University of Aveiro, 3810-193 Aveiro, Portugal

[2]Department of Physics, IMARENAB, University of León, 24071 León, Spain

[3]Droplet Measurement Technologies, Boulder, CO, USA

[4]Institute of Environmental Assessment and Water Research, Spanish Research Council, 08034 Barcelona, Spain

[5]Swedish National Road and Transport Research Institute (VTI), SE-581 95 Linköping, Sweden

Abstract

A road simulator was used to generate wear particles from the interaction between two tyre brands and a composite pavement. Particle size distributions were monitored using a scanning mobility particle sizer and an aerosol particle sizer. Continuous measurements of particle mass concentrations were also made. Collection of inhalable particles (PM_{10}) was conducted using a high-volume sampler equipped with quartz filters, which were then analysed for organic and elemental carbon, organic constituents and elemental composition. Tyre fragments chopped into tiny chips were also subjected to detailed organic and elemental speciation. The number concentration was dominated by particles < 0.5 μm, whereas most of the mass was found in particles > 0.5 μm. The emission factor from wear between pavements and tyres was of the order of 2 mg km^{-1} veh^{-1}. Organic carbon represented about 10% of the PM_{10} mass, encompassing multiple aliphatic compounds (*n*-alkanes, alkenes, hopanes, and steranes), PAHs, thiazols, *n*-alkanols, polyols, some fragrant compounds, sugars, triterpenoids, sterols, phenolic constituents, phthalate plasticisers and several types of acids, among others. The relationship between airborne particulate organic constituents and organic matter in tyre debris is discussed. The detection of compounds that have been extensively used as biomass burning tracers (e.g. retene, dehydroabietic acid and levoglucosan) in both the shredded tiny tyre chips and the wear particles from the interaction between tyres and pavement puts into question their uniqueness as markers of wood combustion. Trace and major elements accounted for about 5% of the mass of the tyre fragments but represented 15 to 18% of the PM_{10} from wear, denoting the contribution of mineral elements from the pavement. Sulphur and zinc were abundant constituents in all samples.

Keywords: non-exhaust emissions, tyres, PM_{10}, size distributions, organic compounds, elements

Introduction

Air pollution is a global environmental problem and the subject of increasing worldwide public health concern. More than 80% of people living in urban areas that monitor air pollution are exposed to air quality levels that exceed the World Health Organisation (WHO) guidelines. It has been clearly demonstrated that,

in addition to chronic and acute respiratory diseases, deterioration of urban air quality, specially by rising levels of atmospheric particulate matter (PM), increases the risk of cardiovascular diseases and stroke (Lee et al., 2014, 2018; Newby et al., 2015; Shah et al., 2015), central nervous system diseases (Babadjouni et al., 2017; Block et al., 2012; Sram et al., 2017), and neurodevelopmental and neurodegenerative diseases (Attademo and Bernardini, 2017; Chen et al., 2017; Gao et al., 2017). In October 2013, the International Agency for Research on Cancer (IARC) has classified outdoor air pollution as carcinogenic to humans (Group 1). Particulate matter was evaluated separately and also classified in Group 1. About 15% of all lung cancer worldwide was attributable to particulate air pollution (Loomis et al., 2014).

Lelieveld et al. (2015) used a global atmospheric chemistry model to investigate the link between premature mortality and seven emission source categories in urban and rural environments. They estimated that outdoor air pollution, mostly by PM < 2.5 μm ($PM_{2.5}$), the principal environmental risk factor of death, leads to 3.3 million premature deaths per year worldwide. The Health Effects Institute (2017) estimated this impact in 4.2 million deaths per year, and ranked it 5th worldwide among all risks, including smoking, diet, and high blood pressure. In a more recent paper, Lelieveld et al. (2019) provided new data based on novel hazard ratio functions suggesting that the health impacts attributable to ambient air pollution in Europe are substantially higher than previously assumed. The annual excess mortality rate from ambient air pollution was estimated to be 790,000, from which 40-80% are due to cardiovascular events, which dominate health outcomes. These estimates exceed previous analyses, such as the Global Burden of Disease for 2015, by more than a factor of two.

Road traffic emissions are known to represent a large contribution to PM concentrations in urban areas worldwide (Amato et al., 2016; Karagulian et al., 2015; Pant and Harrison, 2013). In urban areas, proximity to vehicle emissions poses a significant risk to human health, leading to the need for a detailed characterisation of particulate pollution from this source (Kumar et al., 2014; Uherek et al., 2010). The European Union has adopted increasingly stringent regulations to control the composition of exhaust emissions within the vehicle type approval process, because of the implication of road transport as a major source of air pollution. While stringent policies have led to sizeable reductions in exhaust emissions, currently, non-exhaust emissions from road vehicles, which include particles from brake (pads and disks) and tyre wear and pavement abrasion, are still unabated (Amato, 2018; Chang et al., 2012; Thorpe and Harrison, 2008; van der Gon et al., 2013). Data from European cities showed that exhaust and non-exhaust sources contribute equal amounts to total traffic-related emissions (Amato et al., 2014, 2016; Querol et al., 2004), but recent estimates suggest that in the near future about 90% of road traffic emissions will originate from non-exhaust sources (Padoan and Amato, 2018; Pant and Harrison, 2013; van der Gon et al., 2013). It has become more evident that wear particles from road pavements and tyres may contribute to very high levels of inhalable particles in outdoor air, especially in traffic-impacted environments (Chang et al., 2012; Grigoratos and Martini, 2014; Harrison et al., 2012; Hosiokangas et al., 2004; Luhana et al., 2004; Swietlicki et al., 2004).

In many countries, non-exhaust particles are an important research field due to the lack of knowledge, the complex formation and emission processes and their relevant contribution to ambient levels (van der Gon et al., 2013). Quantification of the mass contribution of non-exhaust particles to the ambient levels is challenging, depending upon the use of chemical tracers, which are scarcely characterised. Tyres have been

pointed out as one of the main sources of Zn in urban environments (Harrison et al., 2012; Hjortenkrans et al., 2007), but multiple possible contributions from other sources to this metal in PM raises doubts about its suitability as a tracer (Calvo et al., 2013). Zn is abundant in the road environment and may originate in pavement, as well as in corrosion of cars and road/street equipment (crash barriers, lampposts, etc.) (Fry et al., 2008). Tyre wear is a substantial contributor of PM_{10} emissions, with annual losses of rubber from tyres in Europe estimated to be several thousands of tons (Kole et al., 2017; Pant and Harrison, 2013). Although dominant, almost nothing is known about the carbonaceous fraction of tyre wear particles. Benzothiazoles have been suggested as tracers (Wik and Dave, 2009), but further confirmation is needed. It was also found that tyres may be a source of carcinogenic dibenzopyrenes (Sadiktsis et al., 2012). Furthermore, it has been observed that organic compounds in tyre particles induce reactive oxygen species and heat-shock proteins in human alveolar cell lines (Gualtieri et al., 2008). Toxicological tests exhibited at least as high inflammatory potential for road and studded tyre wear related PM_{10} as from diesel particles (Gustafsson et al., 2008). Recently, tyre wear has also been identified as one of the major contributors to microplastic emissions, which further increases the need for research to characterise wear particles, and their fate and effects, including not only the atmospheric environment, but also aquatic ecosystems (Kole et al., 2017, Wagner et al., 2018). The chronic toxicity of tyre and road wear particles to water- and sediment-dwelling organisms has been assessed in a few studies (Marwood, 2011; Panko et al., 2013a).

Wear particles from tyre/pavement interaction normally range from a few nanometres to micrometric sizes (Dahl et al., 2006; Grigoratos et al., 2018; Kole et al., 2017). Particles from tyre wear are produced either by shear forces between the tread and the road pavement or by volatilisation. While the first process is mechanical and generates mainly coarse particles (Kreider et al., 2010), the second is thermo-mechanical, leading to aerosols mostly in the submicronic mode. In fact, local hot spots on the tread can reach high temperatures, resulting in evaporative losses of the volatile content of tyres (Mathissen et al., 2011). Meta analyses indicate that the coarse PM fraction ($PM_{2.5-10}$) seems stronger related to respiratory disease while the finer fractions tend to be more significantly connected to cardiovascular disease and mortality (Brunekreef and Forsberg, 2005). Site specific studies in areas with high road traffic resuspension (Perez et al., 2009) also found high cardiovascular and cerebrovascular mortality outcomes for $PM_{2.5-10}$, as well as a relation to daily mortality (Meister et al., 2012). It has been observed that ultrafine particles are emitted at higher speeds, higher slip angles and higher longitudinal forces (Foitzik et al., 2018). In fact, the mass and particle number distributions of tyre wear particles largely depend not only on the driving conditions, but also on the type of tyres (studded winter tyres, studless winter tyres, all-season tyres, summer tyres) and pavements (flexible versus rigid) (Gustafsson et al., 2008; Kole et al., 2017; Kreider et al., 2010; Lee et al., 2013; Sjödin et al., 2010).

Improved information about wear particle emissions and their physico-chemical properties from the interaction between tyres and pavements is important not only to infer the health effects, but also to devise source-oriented mitigation measures, and to model source contributions. This work was carried out in a road simulator with the objective of studying wear particle emissions and their properties, including size distributions and a detailed chemical characterisation of both organic and inorganic constituents, as well as the relationship with the chemical composition of the tyres.

Methodology

The road simulator of the Swedish National Road and Transport Research Institute (VTI) was used to generate wear particles with very low contamination from ambient particles and no contamination from exhaust pipes, since the system is electrically actuated (Dahl et al., 2006; Gustafsson et al., 2008, 2009). The road simulator runs four wheels around a circular track with a diameter of 5.3 m. In order to minimise the contribution from resuspension, the simulator hall, including the track and the machine, were subjected to high pressure water cleaning and allowed to dry until the tests were performed. A composite pavement ring, which included 14 different asphalt pavements with distinct rocks and constructions (asphalt concrete, stone mastic asphalt, etc.), was used for the tests. Two different types of summer tyres were tested: i) Michelin Energy Saver (type 1), and ii) Bridgestone Turanza ER300 (type 2).

A scanning mobility particle sizer (SMPS), composed of a differential mobility analyser (DMA, model 3071, TSI Inc., USA) and a condensation particle counter (CPC, model 3010, TSI Inc. USA), was used to obtain particle size distributions between 14 and 660 nm. An aerodynamic particle sizer (APS, model 3321, TSI Inc. USA) was installed to monitor aerosols from 0.54 to 10 µm. To be able to detect short time variations, mass concentration of PM_{10} was monitored with both a DustTrak instrument (TSI Inc. USA) and a tapered element oscillating microbalance (TEOM, Series 1400a, Thermo). High-volume quartz filter (Pallflex®) PM_{10} samples (EcoTech HiVol 3000) were collected during several hours of running the road simulator at 70 km h^{-1}. The road simulator is not designed for fast acceleration or braking. Thus, the highest achievable speed was chosen to generate as much tyre wear as possible. Measurements were made over a period of 5 days with total kilometres per test ranging from 250 to 500. Each test lasted between 2 and 7 hours. The background air was monitored before road testing.

After sampling, circular punches from the quartz filters were analysed for organic and elemental carbon (OC and EC) by a thermal-optical technique (Pio et al., 2011). This technique relies on the quantification of the CO_2 released from the volatilisation and oxidation of different carbon fractions under controlled heating by a non-dispersive infrared (NDIR) analyser. A laser beam and a photodetector are used to measure the filter light transmittance, allowing the separation between the EC formed by OC pyrolysis from the one that was originally in the sample. Carbonate carbon (CC) was determined in a measurement set-up comprising four components: a mass flow meter, a reaction cell, a NDIR CO_2 analyser, and a computer terminal for data acquisition. A portion of each filter (9 mm punches) was acidified with orthophosphoric acid (20%) in a CO_2 free gas stream to convert CC into CO_2, which was then detected by the infrared analyser.

After the experiments with the road simulator, rubber fragments were cut from the tyres and chopped into tiny chips for further organic speciation by gas chromatography-mass spectrometry (GC-MS), following the same methodology applied to 350 cm^2 of each one of the PM_{10} filters. Samples were extracted by refluxing dichloromethane (300 mL) for 24 h and then three times with methanol in an ultrasonic bath (25 mL for 10 min, each extraction). After each extraction, the extracts were combined and filtered. The total organic extracts were then concentrated by rotary evaporation and, finally, separated into five different organic fractions of increasing polarity by flash chromatography on a silica gel column (activated at 150 °C for 3 h). After each elution, the different organic fractions were vacuum concentrated and dried by nitrogen blow

down. The more polar organic compounds were silylated before chromatographic analysis. A detailed description of the entire procedure was previously provided by Alves et al. (2011).

Six circular punches (3.3 cm diameter) of each filter and tyre rubber fragments were also subjected to acid digestion in closed Teflon 60 mL reactors with a $HF:HNO_3:HClO_4$ mixture, then evaporated, and finally re-dissolved with HNO_3 (Querol et al., 2001). The resulting solutions were analysed for about 60 elements by inductively coupled plasma atomic emission spectroscopy (ICP-AES) and inductively coupled plasma mass spectroscopy (ICP-MS).

3. Results and Discussion

3.1. Particle concentrations and size distributions

A TEOM, DustTrak, APS and SMPS were employed during the experiments. However, only the APS and SMPS were in operation during the entire five-day period. In addition, comparisons of the mass concentrations derived with the DustTrak and APS, with those from the TEOM, brought into question the reliability of the DustTrak measurements. Thus, the DustTrak acquisitions were not subsequently used in the analysis. Instead, the mass concentrations were derived from the APS and SMPS size distributions assuming a particle density of 1.8 g cm^{-3}. Figure 1 shows the time series of mass concentrations measured in each of the five days. Filters were exposed during the time periods enclosed by the red dotted boxes. The mass derived from the SMPS is not shown in this figure because it contributes to less than 1 % of the total mass.

As seen in Figure 1, panels C-E, the TEOM and APS mass concentrations were in reasonable agreement, even though the TEOM measurements appear more variable on April 17 than those of the APS. Given that the TEOM was only operated on the last three days, and that the APS-derived mass concentrations are in good agreement with those from the TEOM (Fig. S1), the results from APS will be reported here for the purpose of comparing tyre brands and distances travelled during the tests.

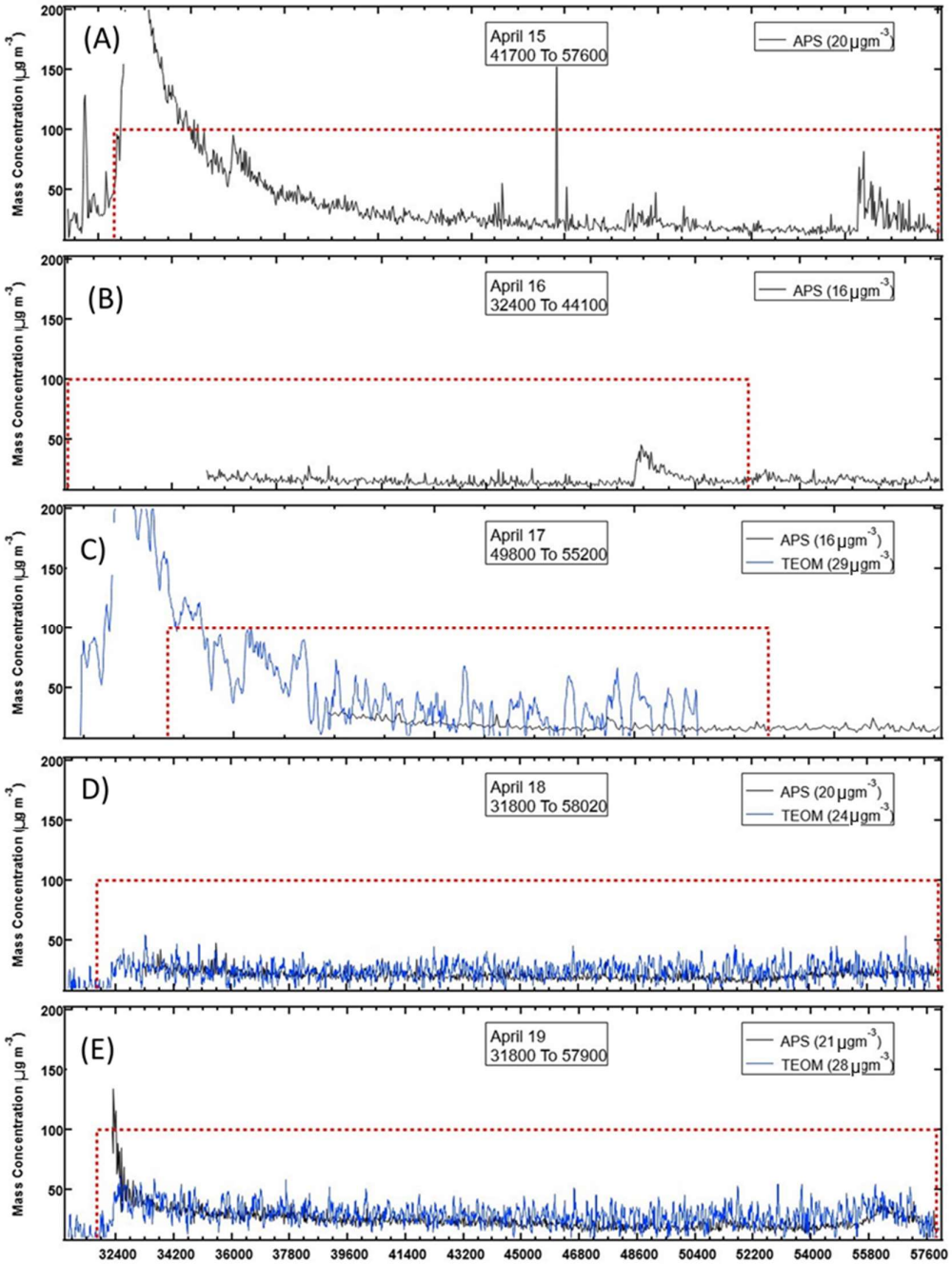

Figure 1. Mass concentration time series for April 15-19 (Panels A-D). Only the APS (black curve) and SMPS (not shown) were in operation on April 15 and 16. The TEOM (blue curve) was operated on April 17-19 (Panels C-D). The red dashed boxes show the period when filter samples were collected.

Figure 2 shows the number (Fig. 2A) and mass (Fig. 2B) concentration size distributions measured by the SMPS and APS. The number concentration is dominated by particles < 0.5 µm, whereas most, i.e. > 99%, of the mass is found in particles > 0.5 µm. The size distributions of the number concentrations revealed a few differences between the conditions tested. The concentration of particles between 0.02 and 0.5 µm was significantly higher for the Michelin tyre during the second day of testing when it travelled its longest distance (448 km). The 1st day of testing of the Bridgestone tyre showed a large peak at 0.025 µm that is not seen in any of the other tests, regardless of distance or tyre type. The size distribution from the last day of

testing of the Bridgestone tyre displayed a much smaller concentration of particles < 0.5 μm than any of the other tests, even though this was the longest distance for this tyre.

The mass size distributions exhibit some differences, such as the lower mass concentrations between 0.7 and 2 μm for days 1 and 2 of the Michelin tyres compared to the 3rd day of this brand that matched the mass measured during all three days from the Bridgestone. Although some variations in masses have been observed for sizes larger than 2 μm, there seems to be no systematic difference that can be clearly linked either to the type of tyre or the distance travelled. For Michelin tyres, the average mass concentrations were 20, 26 and 16 μg m^{-3} for distances travelled of 300, 396 and 448 km, respectively. For Bridgestone, these numbers were 16, 20 and 21 μg m^{-3} for distances travelled of 396, 481 and 496 km, respectively. Although the differences in distance travelled were more for the Michelin than the Bridgestone, there are no trends that would suggest that distance travelled is a factor in particle mass produced. It should be born in min, however, that distances travelled differ only a few tens or hundreds of kilometres, which is manifestly little to draw conclusions.

Depending on the vehicle speed, Lee et al. (2013) obtained non-exhaust PM_{10} concentrations between 31.9 and 49.9 μg m^{-3} using a mobile measurement system. Kim and Lee (2018) reported PM_{10} concentrations from approximately 3 to 39 μg m^{-3} under a constant speed of 110 km h^{-1} in a tyre simulator operated with lateral loads ranging between 500 and 2500 N. A linear relationship between loads and PM_{10} concentrations was clearly observed. Much higher PM_{10} concentrations, up to about 5 mg m^{-3}, were obtained in the same road simulator of the present study using studded tyres (Gustafsson et al., 2008). The results showed that studded tyres produce tens of times more particles than friction tyres. PM_{10} concentrations ranging from 0.44 to 6.48 mg m^{-3} were reported by Kupiainen et al. (2005) for the same test facility. The lowest concentrations and emission factors were measured with low speed (15 km h^{-1}), non-studded tyres, and without traction sand on the pavement, and the highest were obtained with high traction sand loads.

(A)

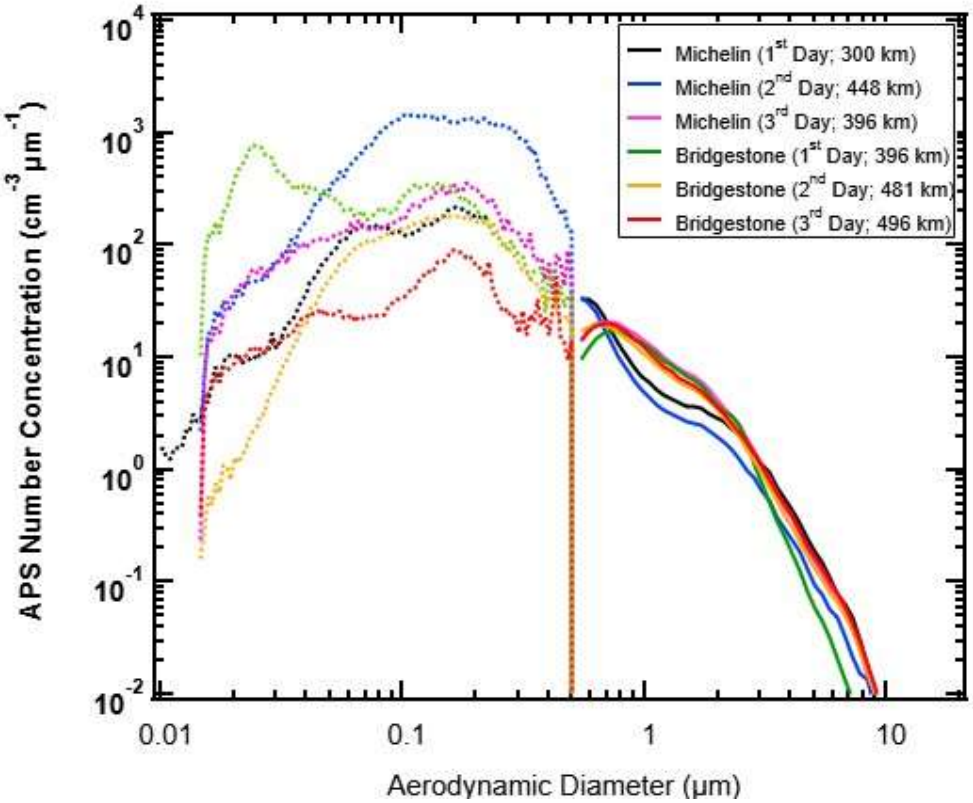

(B)

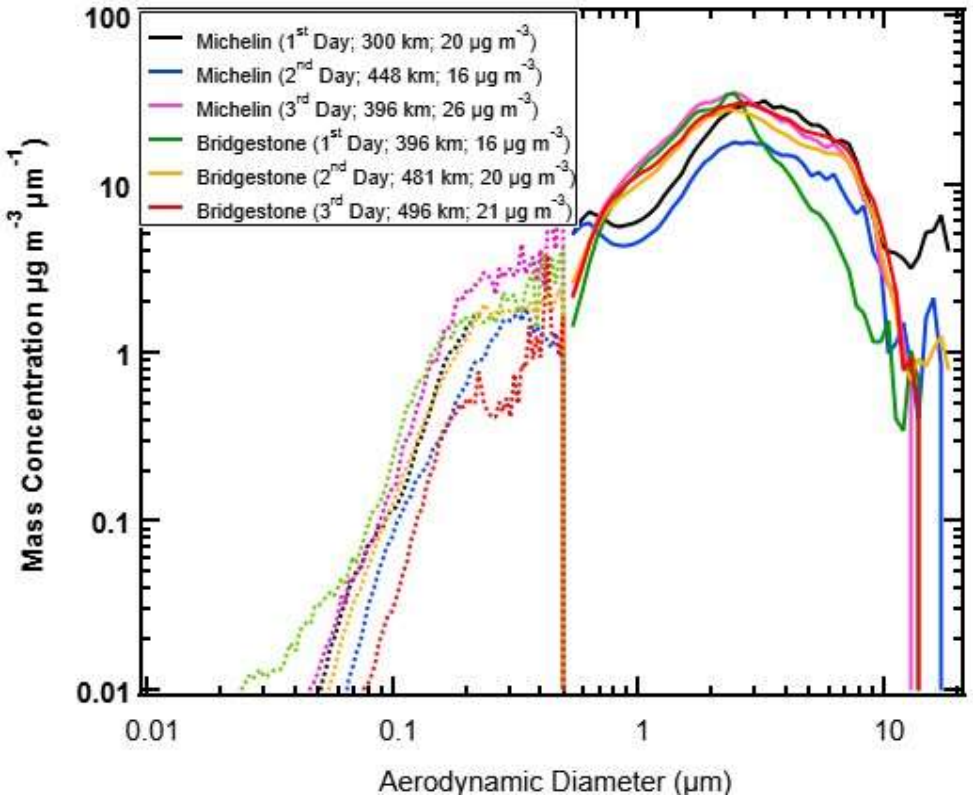

Figure 2. Number (A) and mass (B) concentration measured with the SMPS (dashed curves) and APS (solid curves) size distributions highlighting differences related to distance travelled by the same type of tyres (Michelin and Bridgestone).

The overall mass size distributions of tyre wear particles have been reported to span from < 5 to more than 300 µm (Cadle and Williams, 1979). Kreider et al. (2010) reported a wide unimodal size distribution, as measured by laser diffraction, from 5 to 220 µm, with a mode centred at around 75-100 µm, and only a very small fraction for particles < 10 µm. Other studies explored the size distribution of the airborne fraction of tyre wear particles, and the results indicate that these distributions vary with the tyre and pavement type. Studless tyres were found to generate both unimodal (2.5 µm) and bimodal distributions with modes ranging between 0.3-5 µm and 4-10 µm (Grigoratos and Martini, 2014; and references therein). When studded tyres were used, a bimodal mass size distribution (1.0 and 10 µm) was observed but, at higher speed, a unimodal distribution at 9-10 µm was also registered (Kupiainen et al., 2005). Unimodal distributions were also reported at 3-4 µm by Sjödin et al. (2010). Concerning the contribution to ambient PM_{10}, data from Amato (2018), and references therein, evidence that 60% of the mass of tyre wear particles ranged in size from 2.5 to 10 µm, with APS data showing a bimodal mass size distribution, with peaks around 1 µm and between 5-8 µm.

Once the experiments have started, the PM_{10} concentration increased from about 20 µg m^{-3} to > 200 µg m^{-3}, approximately 20 min later, as shown in panels A and C of Figure 1. The initial peak is probably caused by particles that have not been removed from the track/pavement despite careful cleaning. Afterwards, the concentrations stabilised due to the equilibrium between generation and deposition of particles. An emission factor (EF) was calculated for the tests of April 15 using the simple box model of Dahl et al. (2006), which assumes that the concentration in the test chamber reaches an equilibrium value when emissions are balanced by sedimentation. The mass emission rate, Q, is determined by fitting the following equation to the measurements:

$$M(t)=M_0\, e^{-Kt} + (Q/K)(1- e^{-Kt}) \qquad (1)$$

where 1/K represent the response time, τ.

In this example, the mass emission rate was 0.04478 µg m^{-3} s^{-1}, which corresponds approximately to 1.9 mg km^{-1} veh^{-1} (Fig. 3), when considering the sampling time, volumetric flow rate and velocity of the vehicle. This value is close to the EF of 3.8 mg km^{-1} veh^{-1} obtained for summer tyres by Sjödin et al. (2010), but lower than the EF of 9.0 mg km^{-1} veh^{-1} reported by Kupiainen et al. (2005) for friction tyres. When using non-studded tyres, a high proportion of the tyre road wear particles formed is tyre wear, while the contribution from the pavement itself is low and therefore of less importance for an emission factor. Pavement samples in the road simulator of the present study are all asphalts, but with varying recipes used. They have similar durability and will wear similarly. Nevertheless, the estimated emissions are, of course, specific for this mixed pavement ring and calculated emission factors should be realistic for any stone mastic asphalt (SMA) pavements with similar durability.

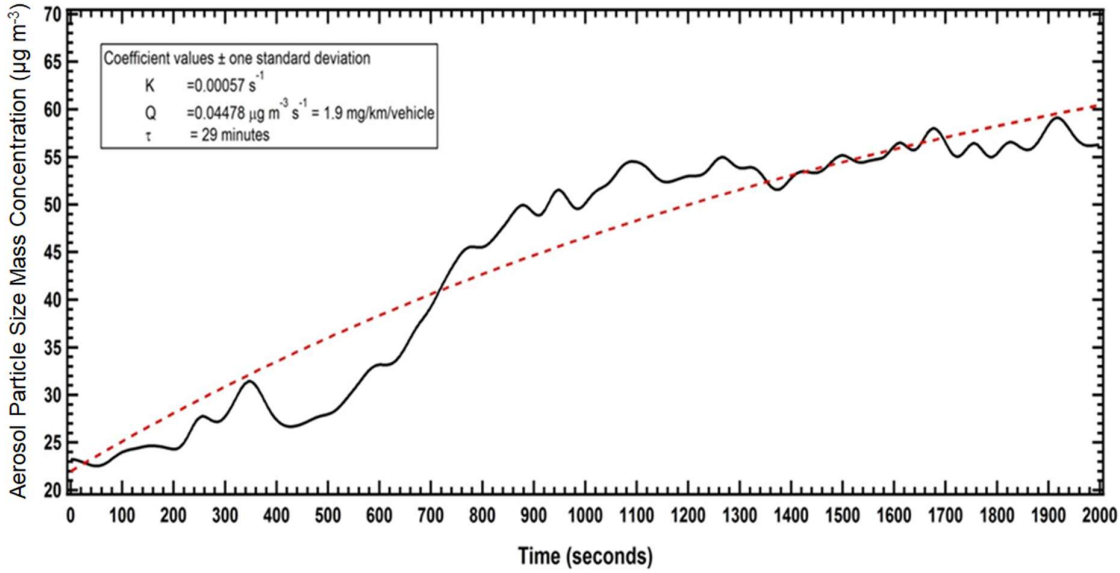

Figure 3. An example of the mass concentration measured by the APS (0.54 – 10 µm) at the beginning of the road test. The dashed line is the best fit of the box model equation, where K and Q are the independent variables.

It should be noted that EFs and chemical characteristics of non-exhaust particles from tyre-road interaction depend on several factors, including load on tyre, life of tyre (i.e. km travelled, both total and in the trip), tyre pressure, speed, road surface type, friction, contact area, among others (Aatmeeyata et al., 2009; and references therein). Thus, emissions obtained in this study should be regarded as representative of non-studded tyre wear under specific experimental conditions.

3.2. Chemical composition of wear particles and tyres

3.2.1. Carbonaceous speciation

Carbonate carbon accounted for PM_{10} mass fractions around 1% (Table 1 and Fig. S2). In addition to a probable origin in the pavement, it is also possible that part of the CC comes from the rubber of the tyres. Some manufacturers describe calcium carbonate as a reinforcing filler to improve strength and to impart stiffness to non-cured rubber. Regardless of the tyre type, OC represented about 10% of the PM_{10} mass, whilst the EC contribution was markedly lower and more than twice in one case as compared to the other (3.3 and 1.5%). From the thermograms, it was observed that 56% (PM_{10} from Tyre 1) and 60% (PM_{10} from tyre 2) of the OC was the fraction that volatilises at high temperature (200-600ºC), comprising the high molecular weight and highly branched compounds. Park et al. (2017) analysed the carbonaceous content of tyre powder produced by mechanical abrasion. The results indicated that 72.4% of the tyre consisted of carbonaceous materials. Among these, 75% of the carbon could be classified as OC (54% of the total tyre) and the remaining 25% was EC (18% of the total tyre). The EC in tyre wear particles originates largely from the carbon black, which is added as a filler to make the tyre UV-resistant, accounting for weight percentages of 22-40% (Kole et al., 2017). The organic fraction of atmospheric PM from tyre wear is related to the

general composition of rubber blends commonly used in passenger vehicles: natural rubber (40%), styrene-butadiene rubber (30%), butadiene rubber (20%) and other rubber (10%) (Grigoratos and Martini, 2014). It has been argued that the plausible mechanism of the PM formation is a combined process of volatilisation and condensation of organic compounds (Park et al., 2017). Aatmeeyata and Sharma (2010) observed that, on average, artificially abraded tyre particles, using a stainless-steel file, had 65.2% carbon, of which, 40.8% was OC and 24.4% was EC (OC:EC ratio ~1.6-1.7). In a simple experimental set-up, the same researchers collected large particles (> 10 μm) from tyre and road wear due to rolling friction. It was observed that the carbon contents in particles from tyre/concrete interaction were lower than those in abraded tyre particles, given that the former also include road wear. In a similar test facility as in the present study, and depending on type of tyre, properties of traction sand aggregate and driving speed, Kupiainen et al. (2005) obtained OC and EC weight percentages in PM_{10} ranging from 2.8 to 8.3% and from < 0.1 and 1.4%, respectively.

Table 1. Concentrations of wear particles collected on high-vol filters from pavement/tyre interaction and their carbonaceous content (TC = total carbon)

	Wear particles from tyre type 1	Wear particles from tyre type 2
PM_{10} (μg m^{-3})	35.4	30.3
CC (wt%)	0.761	1.36
OC (wt%)	10.4	10.3
EC (wt%)	3.26	1.48
TC (wt%)	14.4	13.1
OC:EC	3.19	6.96

The aliphatic organic extracts comprised *n*-alkanes, some alkenes, hopanes and steranes. The dominant *n*-alkane in PM_{10} samples was undecane (Table 2). However, due to its semi-volatility, the mass fractions should be regarded as indicative. Excepting this compound, the homologous series were dominated by C_{25} to C_{35} members, with even-numbered carbon prevalence. Boulter (2006) suggested that *n*-alkanes > C_{35} would be useful marker for tyre wear, since these aliphatics have very few urban emission sources other than rubber wheel abrasion. The detection of homologues generally only up to C_{35} in either the PM_{10} samples or the tyre extracts contradicts this assumption. Moderate to good correlations were obtained between *n*-alkane mass fractions in tyres and the OC-normalised concentrations in PM_{10} (Figure S3). *n*-Alkanes are added to the tyre stock solution as agents to protect the rubber material from oxidants and UV-light induced cracking, playing a role similar to that of natural leaf waxes (Rogge et al., 1993).

Significant unresolved complex mixtures (UCM), composed of numerous branched and cyclic hydrocarbons, were observed in all samples: 618 mg g^{-1} OC (PM_{10} of tyre 1), 254 mg g^{-1} OC (PM_{10} of tyre 2), 40.9 mg g^{-1} OC (tyre 1), and 49.6 mg g^{-1} OC (tyre 2). Most of these unresolved compounds probably originated from the large molecules that make up the tyres. The magnitude of this contribution is also demonstrated by the high ratios between the unresolved to resolved components (U/R): 36, 16, 10 and 33, respectively.

Table 2. Mass fractions of aliphatic compounds in PM_{10} and tyre samples

	PM_{10} from tyre type 1 (µg g^{-1} OC)	PM_{10} from tyre type 2 (µg g^{-1} OC)	Tyre type 1 (µg g^{-1})	Tyre type 2 (µg g^{-1})
n-ALKANES				
n-Decane	-	-	-	-
n-Undecane	14,334	21,429	262	318
n-Dodecane	239	445	5.12	3.31
n-Tridecane	0.010	10.1	0.00	3.26
n-Tetradecane	-	9.24	1.85	1.05
n-Pentadecane	-	25.5	1.96	1.09
n-Hexadecane	5.96	42.9	3.88	1.98
n-Heptadecane	86.9	58.2	2.17	2.86
n-Octadecane	385	87.0	4.59	6.54
n-Nonadecane	241	105	5.12	9.22
n-Eicosane	226	113	5.79	17.8
n-Heneicosane	725	131	6.98	25.9
n-Docosane	326	230	17.4	36.7
n-Tricosane	412	336	35.2	50.5
n-Tetracosane	761	342	25.3	51.5
n-Pentacosane	2,030	3,486	29.3	61.8
n-Hexacosane	670	128	46.0	49.4
n-Heptacosane	598	32.8	54.3	45.7
n-Octacosane	1,248	471	70.8	59.1
n-Nonacosane	1,988	758	61.7	42.8
n-Triacontane	3,117	582	134	71.2
n-Hentriacontane	3,195	1,213	225	128
n-Dotriacontane	2,904	1,407	220	93.4
n-Tritriacontane	1,647	930	127	56.7
n-Tetratriacontane	7,420	4,884	1,806	-
n-Pentatriacontane	560	3,508	249	-
n-Hexatriacontane	-	-	-	-
n-Heptatriacontane	31.2	-	-	-
n-Octatriacontane	-	-	-	-
Σalkanes	**43,150**	**40,764**	**3,401**	**1,138**
ALKENES				
1-Tetradecene	834	1015	16.7	19.9
Hexadecene	-	19.8	1.34	1.67
1-Octadecene	383	1.13	-	-
Eicosene	15.3	28.5	-	-
9-Tricosene	20.9	125	-	-
Squalene	-	117	-	-
Dodecene	758	1143	15.8	17.2
Tritriacontene	-	58.8	6,046	1,534

Note: The dash means not detected

Hopanes, generally pointed out as markers of primary particle emissions from lubricating oils or coal combustion (Alves et al., 2017), were detected and quantified by the key ion *m/z* 191 at mass concentrations of 0.953-1.39 mg g^{-1} OC and 266-356 µg g^{-1} in PM_{10} and tyre samples, respectively (Table 3). As far as we know, only Rogge et al. (1993) have documented the presence of a few pentacyclic triterpanes in fine tyre wear particles (684 µg g^{-1}). The detection of these compounds in non-exhaust emissions puts into question their common utilisation as biomarkers of fossil fuel combustion. The presence and formation processes of

these compounds in the tyre material and in particles resulting from tyre friction on pavements requires further studies. As previously observed (Alves et al., 2017), ratios between hopanes overlap with those of other sources, indicating that these diagnostic tools cannot be used to differentiate the contribution of tyre wear from that of fossil fuel burning. Good correlations between the mass concentrations in tyres and the OC-normalised concentrations in PM_{10} (Figure S3), suggest a major origin in the rubber constituents of the wheels. Hopanoids possibly derive from polymeric synthetic rubbers or some specific chemical fillers made from petroleum, which are nowadays added to the tyres. Some hopanoids were only detected in wear particles from the interaction between tyres and pavements. This may point to an additional origin from the asphalt pavement. However, other compounds were only present in tyre tread samples.

Table 3. Mass fractions of hopanoid and triterpenoid compounds in PM_{10} and tyre samples

	PM_{10} from tyre type 1 (µg g^{-1} OC)	PM_{10} from tyre type 2 (µg g^{-1} OC)	Tyre type 1 (µg g^{-1})	Tyre type 2 (µg g^{-1})
C_{19} Tricyclic terpane	-	11.9	-	-
C_{20} Tricyclic terpane	13.4	17.4	-	-
C_{21} Tricyclic terpane	10.6	13.5	-	-
C_{22} Tricyclic terpane	7.46	7.57	-	-
C_{23} Tricyclic terpane	57.9	62.2	6.48	4.25
C_{24} Tricyclic terpane	42.1	43.8	4.51	1.67
C_{25} Tricyclic terpane (R + S)	39.2	42.7	-	-
C_{26} Tricyclic terpane (22R)	17.7	20.6	-	-
C_{26} Tricyclic terpane (22S)	19.8	22.8	4.44	5.05
C_{28} Tricyclic terpane (22R)	13.7	22.1	1.79	1.30
C_{28} Tricyclic terpane (22S)	17.6	21.3	-	-
C_{29} Tricyclic terpane (22R)	14.9	24.5	-	-
C_{29} Tricyclic terpane (22S)	13.0	19.6	-	-
18α(H)-22,29,30-trisnorneohopane	43.3	59.0	8.61	10.2
17α(H)-22,29,30-trisnorhopane	9.83	19.9	-	-
C_{30} Tricyclic terpane (22R)	61.7	75.0	13.8	15.3
C_{30} Tricyclic terpane (22S)	17.0	20.1	3.99	5.68
C_{31} Tricyclic terpane (22R)	15.5	32.7	-	-
C_{31} Tricyclic terpane (22S)	14.7	17.8	-	-
17α(H),21β(H)-30-norhopane	131	217	48.1	48.2
18α(H)-30-norneohopane	41.0	55.2	14.6	10.0
17α(H)-diahopane	142	212	50.7	41.2
17β(H),21α(H)-normoretane	-	-	-	-
17α(H),21β(H)-hopane	-	-	7.57	8.22
17β(H),21α(H)-moretane	-	-	5.21	-
17α(H),21β(H)-22S-homohopane	63.2	97.5	30.1	22.1
17α(H),21β(H)-22R-homohopane	57.0	75.1	22.2	17.3
Gammacerane	-	-	5.31	3.69
17β(H),21α(H)-(22R+22S)-homomoretane	-	-	5.62	3.38
17α(H),21β(H)-22S-bishomohopane	35.0	49.7	19.4	12.1
17α(H),21β(H)-22R-bishomohopane	22.7	40.1	13.6	7.65
17α(H),21β(H)-22S-trishomohopane	19.9	29.6	14.2	7.71
17α(H),21β(H)-22R-trishomohopane	11.8	13.6	9.17	5.05

17α(H),21β(H)-22S-tetrakishomohopane	-	15.2	9.86	4.17
17α(H),21β(H)-22R-tetrakishomohopane	-	9.92	11.1	6.60
Unidentified hopane	-	-	6.20	2.66
Unidentified hopane	-	-	14.0	8.93
17α(H),21β(H)-22S-pentakishomohopane	-	15.7	8.75	4.53
17α(H),21β(H)-22R-pentakishomohopane	-	5.90	11.1	6.11
Unidentified hopane	-	-	5.89	3.32
Σhopanoids and triterpenoids	953	1392	356	266

Note: The dash means not detected or below detection limit.

Monoaromatic (MA, *m/z* 253), triaromatic steranes (TA, *m/z* 231), and steranes (*m/z* 217) are a group of biomarker compounds that are highly resistant to biodegradation and have been used for oil source tracking. The *m/z* 231 mass chromatograms were characterised by series of 20R and 20S C_{26}-C_{27}-C_{28} triaromatic steranes (TA-cholestanes, TA-ergostanes, and TA-stigmastanes) plus C_{20} to C_{22} TA-steranes (Table 4). However, although many triaromatic steranes have been detected in the organic extracts of the two tyre brands, most of the compounds were absent from the PM_{10} samples, suggesting non-emission during the wear process or degradation. The *m/z* 253 mass chromatograms were composed of series of 20R and 20S C_{27}-C_{28}-C_{29} 5β(H) and 5α(H) MA steranes, as well as rearranged ring-C 20S and 20R MA-diasteranes (Table 5). The amount of these compounds in PM_{10} resulting from the wear of tyre type 2 was about twice compared to PM_{10} coming from tyre type 2.

Table 4. Mass fractions of monoaromatic and triaromatic steranes in PM_{10} and tyre samples

Triaromatic steranes, *m/z* 231 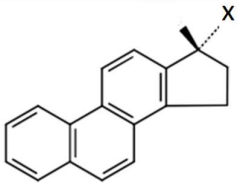	PM_{10} from tyre type 1 (μg g^{-1} OC)	PM_{10} from tyre type 2 (μg g^{-1} OC)	Tyre type 1 (μg g^{-1})	Tyre type 2 (μg g^{-1})
C_{20} TA-sterane (X = ethyl)	6.43	-	19.4	12.9
C_{21} TA-sterane (X = 2-propyl)	7.49	-	16.5	10.0
C_{22} TA-sterane (X = 2-butyl) (epimer 1 at C-19)	-	-	4.87	3.87
C_{22} TA-sterane (X = 2-butyl) (epimer 2 at C-19)	-	-	3.13	2.73
C_{26} TA-chloestane (20S)	-	-	7.61	8.98
C_{26} TA-chloestane (20R) + C_{27} TA-ergostane (20S)	15.7	-	40.8	44.4
C_{28} TA-stigmastane (20S)	-	-	32.2	32.1
C_{27} TA-ergostane (20R)	-	-	26.5	27.0
C_{28} TA-stigmastane (20R)	-	-	21.1	28.2
Σ triaromatic steranes	**296**	**-**	**172**	**170**

Monoaromatic steranes, *m/z* 253 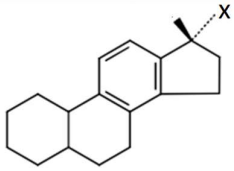	PM_{10} from tyre type 1 (μg g^{-1} OC)	PM_{10} from tyre type 2 (μg g^{-1} OC)	Tyre type 1 (μg g^{-1})	Tyre type 2 (μg g^{-1})
C_{21} MA-sterane (X = ethyl)	-	7.49	4.29	1.66

C_{22} MA-sterane (X = 2-propyl)	-	-	-	-
C_{23} MA-sterane (X = 2-butyl)	-	-	3.58	3.73
C_{27} 5β(H) MA-cholestane (20S)+C_{27} MA-diacholestane (20S)	31.9	52.3	8.49	6.96
C_{27} 5β(H) MA-cholestane (20R)+C_{27} MA-diacholestane (20R)	11.9	25.0	4.83	5.91
C_{27} 5α(H) MA-cholestane (20S)	-	7.38	1.69	2.41
C_{28} 5β(H) MA-ergostane (20S)+C_{28} MA-diaergostane (20S)	33.5	51.0	9.43	8.15
C_{27} 5α(H) MA-cholestane (20R)	20.4	36.1	6.47	6.36
C_{28} 5α(H) MA-ergostane (20S)	31.2	43.1	5.81	6.11
C_{28} 5β(H) MA-ergostane (20R)+C_{28} MA-diaergostane (20R)	14.8	19.3	5.41	4.13
C_{29} 5β(H) MA-stigmastane (20S)+C_{29} MA-diastigmastane (20S)	-	-	1.68	0.89
C_{29} 5α(H) MA-stigmastane (20S)	-	-	2.80	2.22
C_{28} 5α(H) MA-ergostane (20R)	14.3	28.1	9.02	8.42
C_{29} 5β(H) MA-stigmastane (20R)	-	-	1.62	1.48
C_{29} 5α(H) MA-stigmastane (20R)	-	-	1.31	1.74
C_{30} 5β(H) MA-sterane (20S)	-	-	-	-
Σ monoaromatic steranes	**158**	**270**	**66.4**	**60.2**

C-19 is the carbon at the dashed position

Table 5. Mass fractions of steranes (*m/z* 217) in PM_{10} and tyre samples

	PM_{10} from tyre type 1 (μg g^{-1} OC)	PM_{10} from tyre type 2 (μg g^{-1} OC)	Tyre type 1 (μg g^{-1})	Tyre type 2 (μg g^{-1})
C_{20} Sterane	16.8	22.8	6.03	2.93
C_{21} Sterane	-	-	22.81	8.86
C_{22} Sterane	-	-	10.13	5.88
13β(H), 17α(H), 20S-Cholestane (diasterane) (C_{27})	45.5	58.5	4.50	3.70
13β(H), 17α(H), 20R-Cholestane (diasterane) (C_{27})	32.7	38.8	2.66	2.70
13α(H), 17β(H), 20R-Cholestane (diasterane) (C_{27})	20.3	35.5	-	-
13α(H), 17β(H), 20S-Cholestane (diasterane) (C_{27})	51.2	46.1	-	-
13β(H), 17α(H), 20S-Cholestane (diasterane) (C_{28})	18.4	21.7	-	-
13β(H), 17α(H), 20R-Cholestane (diasterane) (C_{28})	8.92	25.2	-	-
ααα (20S)-Cholestane (C_{27})	32.6	58.0	2.63	4.07
αββ (20R)-Cholestane (C_{27})	46.2	62.0	5.06	5.99
αββ (20S)-Cholestane (C_{27})	51.5	62.7	4.26	5.69
ααα (20R)-Cholestane (C_{27})	73.5	87.7	6.86	6.27
24-Methyl-5α(H), 14α(H), 17α(H) 20S-Cholestane (20S,24S) (C_{28})	17.1	35.6	2.02	1.60
24-Methyl-5α(H), 14β(H), 17β(H) 20R-Cholestane (20R,24S) (C_{28})	27.0	54.1	4.27	5.67
24-Methyl-5α(H), 14β(H), 17β(H) 20S-Cholestane (20S,24R) (C_{28})	23.7	51.7	5.09	5.08
24-Methyl-5α(H), 14α(H), 17α(H) 20R-Cholestane (20R,24R/S) (C_{28})	25.4	43.1	5.53	4.28
24-Ethyl-5α(H), 14α(H), 17α(H) 20S-Cholestane (20S,24R) (C_{29})	25.8	46.5	7.86	5.60
24-Ethyl-5α(H), 14β(H), 17β(H) 20R-Cholestane (20R,24R) (C_{29})	24.1	59.7	7.96	4.89
24-Ethyl-5α(H), 14β(H), 17β(H) 20S-Cholestane (20S,24R) (C_{29})	34.1	52.1	11.46	9.90
24-Ethyl-5α(H), 14α(H), 17α(H) 20R-Cholestane (20R,24R) (C_{29})	34.1	50.8	6.73	5.40

C_{30} Sterane	-	-	6.96	6.74
C_{30} Sterane	-	-	6.31	5.34
C_{30} Sterane	-	-	8.37	6.91
Σ steranes	**609**	**912**	**137**	**108**

The dominant PAH was naphthalene, a volatile compound that exists in both gaseous and PM phases (Table 6). Alkyl-PAHs were also present. Fluoranthene, chrysene, pyrene and phenanthrene were abundant in PM_{10}, while chrysene, pyrene, benzo[e]pyrene and benzo[ghi]perylene predominated in tyres. It was reported that PAH emissions increase with increasing mileage of the tyre (Aatmeeyata and Sharma, 2010). Kwon and Castaldi (2012) studied the mechanistic processes associated with PAHs from the thermal degradation of tyres under various atmospheric oxygen concentrations. Extender oils are added to rubber compounds during the production of tyres to achieve acceptable process ability. Before 2010, highly aromatic oils, containing 300-700 mg PAHs kg^{-1}, were commonly employed (Aatmeeyata and Sharma, 2010). After this date, the European Union discontinued the use of extender oils in the manufacturing process with more than 1 mg of benzo[a]pyrene per kg, or more than 10 mg of the sum of other regulated PAHs per kg. Thus, the PAH mass fractions documented in the literature can be very discrepant, depending on whether the tyres were manufactured before or after the ban. Sadiktsis et al. (2012) analysed eight tyres for 15 high molecular weight PAHs and observed a high variability in concentrations. A factor of 22.6 was reported between the lowest and the highest PAH content. The difference in the measured PAH content between summer and winter tyres varied significantly across manufacturers, making estimates of total vehicle fleet emissions very ambiguous. The PAH concentrations in the analysed tyres ranged from 3.79 ± 0.54 to 85.2 ± 7.5 μg g^{-1}. Almost all (92.3%) of the total extractable PAH content was ascribed to five compounds: benzo[ghi]perylene, coronene, indeno[1,2,3-cd]pyrene, benzo[e]pyrene, and benzo[a]pyrene. Kreider et al. (2010) analysed PAHs in particles produced using different methods, including on-road collection, laboratory generation under simulated driving conditions, and cryogenic breaking of tread rubber. For all PAHs analysed except acenaphthalene, roadway particles contained significantly higher amounts when compared to tyre wear particles. Total PAH concentrations in roadway, tyre wear and tread particles were 305, 12.7 and 16.1 μg g^{-1}, respectively. This indicated a low contribution of tyres to total PAHs in road dust and environmental media. Natural sources, asphalt, automobile exhausts, and fuel combustion products were proposed as alternative sources of PAHs in the environment. Aatmeeyata and Sharma (2010) analysed artificially abraded tyre particles for their PAH content. Only phenanthrene, fluoranthene, pyrene and benzo[ghi]perylene were observed in the extracts. In accordance with previous studies (Boonyatumanond et al., 2007; Gaad and Kennedy, 2003; Rogge et al., 1993), pyrene presented the highest mean concentration (26.4 μg g^{-1}). Llompart et al. (2013) analysed organic chemicals in rubber recycled tyre playgrounds and found that all samples contained total amounts of PAHs between 1.25 and 70.4 μg g^{-1}, but one of them peaked at 178 μg g^{-1}. The most abundant congener was pyrene, with an average concentration of 7.7 μg g^{-1}. Other abundant congeners were naphthalene, phenanthrene, fluoranthene, and chrysene, with average individual concentrations of about 2 μg g^{-1}. The analysis of commercial pavers (recycled rubber tyre tiles) showed surprising results. All samples gave considerably higher PAH concentrations than the playground

410 samples. In 5 out of 7 samples, the total PAH concentration was extremely high, between 2000 and 8000 µg
411 g^{-1}.

412 Retene has been consistently used as a molecular tracer of softwood combustion (Ramdahl, 1983).
413 However, the suitability of this alkylated phenanthrene as a marker of biomass burning in urban areas was
414 questioned by Alves et al. (2016), because it was found to be one of the dominant PAHs in PM samples
415 collected in a road tunnel. It was also present in particles from uncontrolled combustion of shredded tyres in
416 a landfill (Downard et al., 2015). In the present study, retene was observed at comparable mass
417 concentrations to those of other PAHs. Retene in tyre-related samples may originate from the natural waxes
418 and resins (e.g. pine tars) added as softeners and extenders to the recipe of the rubber stock (Rogge et al.,
419 1993). Benzothiazole, previously pointed out as a good tracer for tyre wear particles (Wik and Dave, 2009),
420 was detected at mass fractions of 6.5 µg g^{-1} OC, 11.9 µg g^{-1} OC, 1.60 µg g^{-1} and 1.65 µg g^{-1} in PM_{10} from the
421 wear of tyre 1 and 2 and in the fragments of tyre rubbers 1 and 2, respectively. Since this aromatic
422 heterocyclic compound is semi-volatile, the partitioning between the gas and particle phases is temperature
423 dependent, raising questions about the appropriateness of benzothiazole as a tracer of tyre wear. In addition
424 to benzothiazole, (3H)-benzothiazolone was also detected, but only in samples of tyre fragments at mass
425 fractions of 2.76 (brand 1) and 1.69 (brand 2) µg g^{-1}. Thiazoles are used as vulcanising agents to increase the
426 durability of tyre rubber (Formela et al., 2015).

427

428 Table 6. PAH mass fractions in PM_{10} and tyre samples

	PM_{10} from tyre type 1 (µg g^{-1} OC)	PM_{10} from tyre type 2 (µg g^{-1} OC)	Tyre type 1 (µg g^{-1})	Tyre type 2 (µg g^{-1})
Naphthalene	521	566	11.3	14.1
Acenaphthylene	0.962	-	0.431	1.33
Acenaphthene	70.5	-	0.130	-
Fluorene	-	3.56	0.104	0.145
Methylphenanthrenes	39.2	72.9	18.4	30.7
Dimethylphenanthrenes	-	51.0	56.5	59.6
Phenanthrene	67.3	28.1	0.984	1.35
Anthracene	1.56	-	0.057	0.179
Fluoranthene	130	56.4	1.78	5.10
Pyrene	70.5	31.6	7.20	12.1
Retene	34.4	17.3	3.30	-
Benzo[a]anthracene	20.6	4.92	1.22	0.479
Chrysene	71.1	37.1	12.4	7.44
Benzo[b]fluoranthene	44.0	13.8	1.52	3.71
Benzo[j]fluoranthene	-	-	-	-
Benzo[k]fluoranthene	24.1	5.88	-	-
Benzo[e]pyrene	48.5	17.6	6.13	10.3
Benzo[a]pyrene	31.7	5.53	1.39	2.50
Perylene	3.90	0.616	0.904	1.30

Indeno[1,2,3-cd]pyrene	26.8	7.02	0.816	3.10
Dibenzo[a,h]anthracene	3.23	0.867	0.497	-
Benzo[ghi]perylene	27.2	12.6	5.88	15.5
ΣPAHs	**1,237**	**933**	**131**	**169**

It should be noted, once again, that tyre rubber contains a huge number of components, such as reinforcing agents, activating agents, antioxidants, processing oil, vulcanising agents, and vulcanisation accelerators. Moreover, several patents describing fragrance-emitting rubbers have been published. Natural or synthetic fragrances together with retention agents are added during the manufacturing of tyres in order to maintain their fragrant component even at 170-180ºC, which are the processing temperatures. When the fragrance-emitting rubber is used in a tyre tread, which continues to wear in direct contact with the ground surface, the fragrance is maintained for a long time. Synthetic fragrances can be produced from an aromatic constituent obtained from plant essences, petroleum or coal. Natural fragrances include vegetable and animal components. Many fragrant constituents were present in our samples (e.g. monoterpenes, some ketones, some aromatic acids, cyclic alcohols, phenolics, etc.). In addition, several other classes of oxygenated organic compounds were also detected, including *n*-alkanols, polyols, sugars and anhydrosugars, sterols, triterpenoids, phthalates, phenolics and several types of acids (Table S1 and Fig. 4).

Among *n*-alkanols, hexadecanol (cetyl alcohol) was the most abundant compound in PM_{10} (16 and 17 mg g^{-1} OC). Sorbitol stood out among polyols in aerosol samples (1.31 and 1.02 mg g^{-1} OC). Many types of organic acids were detected: *n*-alkanoic, *n*-alkenoic, di- and tricarboxylic, hydroxy, aromatic, esters, and resin. Resin acids from pine-tree gum-rosin, such as dehydroabietic, are used in the tyre manufacturing process as emulsifying agents. Previous studies documented the presence of resin acids in tyre-tread rubbers and proposed them as potential tyre-wear markers (Kumata et al., 2011; Nolte et al., 2002; Rogge et al., 1993). However, the relative abundances may diverge appreciably due to differences among the disproportionated rosins used by tyre manufacturers. Kumata et al. (2011) observed that resin acids were more abundant in samples collected near traffic sources than in those collected at sites distant from traffic, even those influenced by biomass burning. Although the latter is a major source of resin acids (Gonçalves et al., 2011), it has been suggested that wood smoke is proportionally more enriched in abietic acid as compared to tyre treads, allowing the use of ratios between compounds to differentiate signatures (Kumata et al., 2011). Fatty acids, such as stearic and palmitic, are used as dispersing agents and softeners. These were by far the dominant acids in samples of the present study.

Phthalate plasticisers are employed as softeners to afford elasticity and stickiness to the tyre. Diisobutyl phthalate, dibutyl phthalate and isooctyl phthalate were the dominant compounds in PM_{10} from tyre wear. The fact that the phthalate signatures do not match between tyres and PM_{10} raises the hypothesis of interconversion or chemical alteration during the wear process. Llompart et al. (2013) found diisobutyl phthalate (DIBP), dibutyl phthalate (DBP), and di(2-ethylhexyl) phthalate (DEHP) in rubber recycled tyre playgrounds and pavers. The most abundant congener was DEHP with concentrations between 4 and 64 μg g^{-1} in playground samples, and between 22 and 1200 μg g^{-1} in the pavers.

464 Anhydrosugars are organic compounds with a six-carbon ring structure formed from the pyrolysis of
465 carbohydrates, such as starch and cellulose. In particular, levoglucosan has been extensively used as a
466 chemical tracer to apportion the biomass burning contribution to atmospheric particulate matter (Vicente and
467 Alves, 2018), based on the principle that this is the only emitting source. However, the detection of this
468 saccharide, at appreciable amounts, in both the tyre samples and the wear particles seriously questions its
469 uniqueness as a biomass burning tracer and suggests that its use as a biomass burning tracer be applied with
470 caution and the appropriate caveats. Over the past years, cellulose fibres have been used as reinforcement
471 materials in the rubber industry. These materials are based on wood cellulose that has been treated to
472 disperse easily in rubber compounds during mixing and bond to the matrix rubber during vulcanisation. The
473 heat that this process generates also serves to fuse the tyre's various components together (Haghighat et al.,
474 2007). Although the mechanisms remain to be explained, it is likely that temperatures reached either in the
475 vulcanisation process or in the friction between the tyre and the pavements during vehicle running can
476 convert part of the cellulose fibres into sugars. It should be noted that in the combustion of woody biomass,
477 levoglucosan is preferably formed in more inefficient processes at lower temperatures (Vicente and Alves,
478 2018), compatible with the values reached when tyres are vulcanised.

479

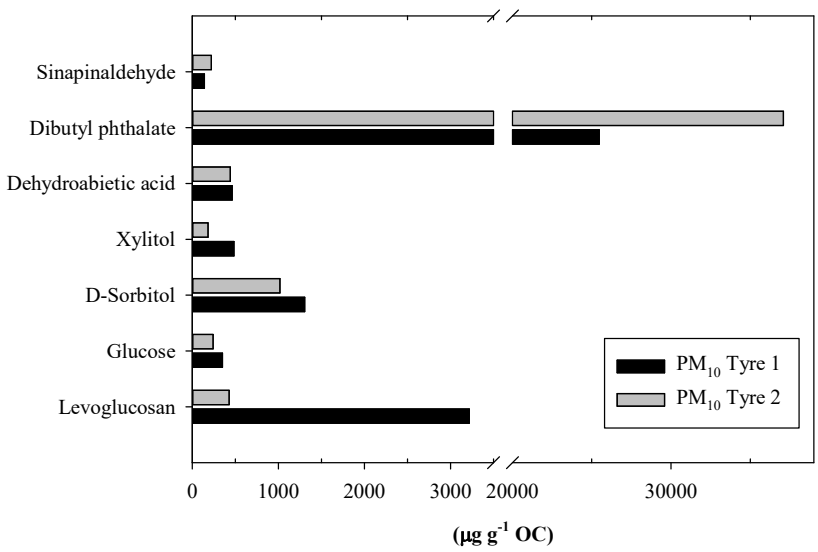

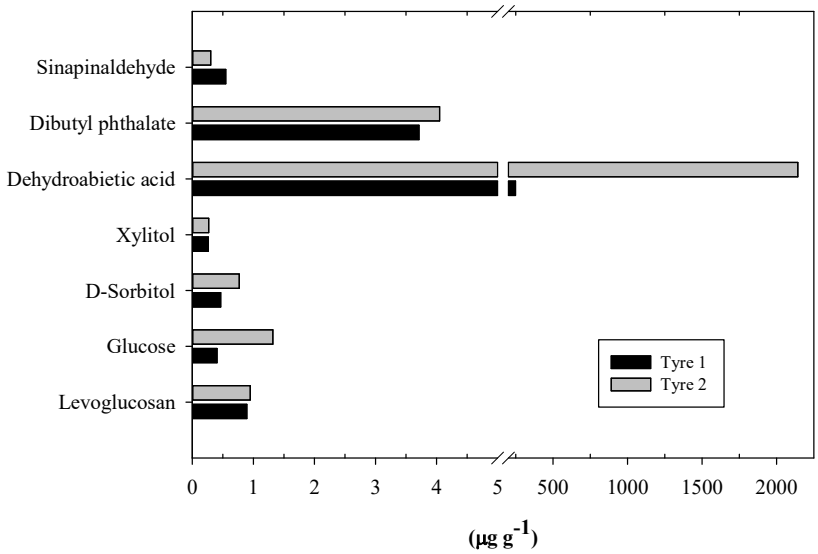

Figure 4. Mass fractions of some of the polar organic compounds detected in both the wear particles and the tyres

3.2.1. Elemental speciation

Trace and major elements from the ICP-MS and ICP-AES measurements accounted for around 5% of the mass of the tyre fragments but represented 15 to 18% of the PM_{10} from wear (Table 7). Similarly to what was concluded by Dall'Osto et al. (2014), this suggests that the interaction of tyres with the road surface creates particles internally mixed from two sources: tyre rubber and road surface materials. Measurements of the tyre rubber component alone may underestimate the contribution of tyre wear to the airborne particulate matter levels.

Al, Ca, Na, Fe and K dominated in PM_{10}, denoting the contribution of mineral elements from the pavement. In the tyre samples, the dominant elements were S and Zn, followed by Na, Al and Ca. Tyre wear particles have been described as a dominant source of Zn to the environment (Councell et al., 2004; Harrison et al., 2012; Pant et al., 2017). Zn is present in tyres either in inorganic forms (ZnS and ZnO) or as organic compound (Zn stearate) (Pant and Harrison, 2013; Wik and Dave, 2009). However, the use of Zn as a tyre wear particle tracer is questionable, since many other sources, such as industrial activities (Lawton et al., 2014), vehicle exhaust (Alves et al., 2015), and engine lubricants (Zmozinski et al., 2010), are also emitters. Sulphur is an important part of tyre composition, acting as a cross-linking agent to confer mechanical strength. Kreider et al. (2010) measured the chemical composition of particles abraded from a tyre, documenting a zinc content of 9000 µg g^{-1}, which was found consistent with previous studies (3000-10,000 µg g^{-1}). In the same work, sulphur was found to be the dominant element in the tyre tread (12,000 µg g^{-1}).

Several other elements have been previously identified in airborne wear particles resulting from the interaction between tyres and pavements (Grigoratos and Martini, 2014; Kreider et al., 2010; Thorpe and Harrison, 2008). The composition of the wear particles may not entirely reflect the original composition of either the tyre treads or the pavements. Due to friction and heat, in comparison with the original tyre tread

and road surface material, the interaction of tyres and pavement modifies the properties of the wear particles (Panko et al., 2013b). However, it is expected that many of the tyre components will be detected in the particulate material. For example, vulcanising agents, which generally make up 1% of the tyre rubber mass, include in their composition S, Se, and Te (durability enhancers), as well as Pb, Mg, Zn, sulphur compounds and calcium oxides (accelerators). Calcium oxides are also used as desiccants, an anti-aging agent of tyre rubber. Gustafsson et al. (2008) tested friction and studded tyres on different pavements and observed that Al and Si were the most abundant elements in airborne wear particles. Kupiainen et al. (2005) also tested studded and friction tyres and wear particles from the interaction with granite pavements. The individual particle analysis with SEM/EDX showed that the majority (over 90 percent) of the particles were aluminosilicates originating from the aggregates used. Such as Zn, Si is a metal found in high abundance in some tyre formulations, due to the use of amorphous silica (SiO_2) in filler materials. Kreider et al. (2010) documented higher Si quantities in road particles (86,000 µg g^{-1}) and tyre wear particles (87,000 µg g^{-1}), when compared to tread particles (54,000 µg g^{-1}). It should be noted that silicon is also found in cement and other road surfaces and is the second most abundant element in the Earth's crust. Thus, the higher proportion of Si in road and tyre wear particles was probably due to its presence in the pavement or environmental dusts from sand or soil. Due to the silica content of quartz fibre filters, Si was not determined in the present study.

Table 7. Mass fractions of elements in PM_{10} and tyre samples

	PM_{10} from tyre type 1 (µg g^{-1})	PM_{10} from tyre type 2 (µg g^{-1})	Tyre type 1 (µg g^{-1})	Tyre type 2 (µg g^{-1})
Li	15.1	16.6	14.6	2.08
Be	1.29	1.27	-	-
B	-	-	23.0	121
Sc	3.61	3.67	-	-
Ti	1,405	1,428	169	47.6
V	46.1	46.8	4.21	6.45
Cr	80.6	75.3	3.98	8.07
Mn	402	471	9.61	3.78
Co	37.2	43.0	2.09	2.67
Ni	36.0	54.4	1.73	0.506
Cu	2,840	2,113	10.8	7.53
Zn	3,321	22,895	13,464	5,893
Ga	10.1	9.82	0.469	0.495
Ge	14.6	18.6	-	-
As	16.9	7.50	-	-
Se	6.83	3.71	-	-
Rb	60.9	64.0	1.66	2.12
Sr	97.3	104	4.61	2.13
Y	15.5	17.5	1.05	0.701
Zr	46.8	1,000	50.0	16.3
Nb	8.84	27.2	1.21	1.55

Mo	93.3	131	0.704	4.64
Cd	2.53	2.49	-	1.32
Sn	36.7	64.1	0.704	2.37
Sb	83.8	56.2	-	1.81
Cs	2.15	2.25	-	-
Ba	405	454	22.4	5.43
La	20.2	26.6	1.51	3.74
Ce	40.8	50.2	2.32	2.78
Pr	4.84	5.24	-	-
Nd	16.4	17.4	1.01	2.89
Sm	3.73	3.94	-	-
Eu	0.598	0.621	-	-
Gd	3.63	4.11	-	-
Tb	0.697	0.699	-	-
Dy	3.24	3.74	-	-
Ho	0.582	0.687	-	-
Er	1.54	1.82	-	-
Tm	1.21	1.37	-	-
Yb	1.48	1.63	-	-
Lu	1.17	1.32	-	-
Hf	0.776	40.5	1.44	-
Ta	1.84	7.37	-	-
W	715	952	7.43	13.5
Tl	2.06	1.25	-	-
Pb	97.7	59.5	1.38	12.2
Bi	1.91	2.21	-	-
Th	9.56	13.9	0.443	-
U	7.91	8.15	-	-
Al	33,944	32,049	2,377	1,882
Ca	23,739	25,259	1,030	2,278
Fe	23,007	37,676	602	712
K	15,891	16,323	373	944
Mg	7,549	7,010	926	415
Na	22,210	24,024	4,286	3,094
P	-	-	22.4	164
S	10,997	8,972	29,926	32,504
wt%	14.7	18.2	5.33	4.82

Note: Cells with dashes mean not detected or below the detection limit

Conclusions

While exhaust emissions will noticeably decrease in the coming years due to more strict regulations, non-exhaust emissions are projected to stay at the same level or increase with traffic volume and will represent a

dominant part of the total PM emissions. This study provides size distributions for wear particles resulting from the interaction between tyres and pavement, as well as the primary PM_{10}-bound chemical composition, including speciated organics and elements. The same chemical constituents were also analysed in the tyre treads. The new databases can help to improve emission inventories and to more accurately apportion the contribution of these non-exhaust source to the atmospheric particulate matter levels. Among the approximately 300 organic compounds analysed, the presence of some of them is documented, as far as we know, for the first time. Good correlations between the mass concentrations of some groups of organic compounds in tyres (e.g. alkanes and hopanes) and the OC-normalised concentrations in PM_{10}, suggest a major origin in the treads. The complex chemical composition of wear particles reflects the wide range of compounds employed in tyre manufacturing. There are many different tyre manufacturers and formulations available all over the world. Consequently, tyre wear particles may also vary in terms of yield, chemical composition and characteristics. Thus, additional studies are needed to obtain a more complete picture.

An overwhelming proportion of the mass emitted from the interaction between tyres and pavement was found in particles > 0.5 μm. The size distributions of number and mass concentrations show day to day differences, as well as some features that differed between the two tyre types; however, the limited number of tyres and distances tested prevent us from reaching specific conclusions that can be applied to a broader population of tyres and environmental conditions. A mass emission factor of the order of 2 mg km^{-1} veh^{-1} was estimated. Given the general agreement on the mass concentrations obtained in the various tests, this mass emission factor can be taken as representative, at least for both tyre brands tested.

It was found that particles from tyre wear are enriched not only in elements that constitute the treads, such as Zn and S, but also in typical mineral elements from the road surface materials. Thus, the contribution of non-exhaust emissions to atmospheric levels from field studies using chemical tracers for particles abraded from tyres may underestimate that arising from tyre-road interaction, unless road wear emission factors are also considered. The detection of retene, resin acids and levoglucosan, either in the tyre treads or in particles from their wear, leads us to question the use of these compounds as unambiguous biomass combustion markers and caution those who use these compounds as tracers to do so with the appropriate caveats.

Acknowledgments

This work was financially supported by the project “Chemical and toxicological SOurce PROfiling of particulate matter in urban air (SOPRO)”, POCI-01-0145-FEDER-029574, funded by FEDER, through COMPETE2020 - *Programa Operacional Competitividade e Internacionalização* (POCI), and by national funds (OE), through FCT/MCTES. Ana Vicente acknowledges the Postdoc grant SFRH/BPD/88988/2012 from the Portuguese Science Foundation and the funding programme POPH/FSE.

REFERENCES

Aatmeeyata, Kaul, D.S., Sharma, M., 2009. Traffic generated non-exhaust particulate emissions from concrete pavement: A mass and particle size study for two-wheelers and small cars. Atmos. Environ. 43, 5691-5697.

Aatmeeyata, Sharma, M., 2010. Polycyclic aromatic hydrocarbons, elemental and organic carbon emissions from tire-wear. Sci. Total Environ. 408, 4563-4568.

Alves, C.A., Barbosa, C., Rocha, S., Calvo, A., Nunes, T., Cerqueira, M., Pio, C., Karanasiou, A., Querol, X., 2015. Elements and polycyclic aromatic hydrocarbons in exhaust particles emitted by light-duty vehicles. Environ. Sci. Pollut. Res. 22, 15, 11526-11542.

Alves, C.A., Vicente, A., Monteiro, C., Gonçalves, C., Evtyugina, M., Pio, C., 2011. Emission of trace gases and organic components in smoke particles from a wildfire in a mixed-evergreen forest in Portugal. Sci. Total Environ. 409, 1466-1475.

Alves, C.A., Vicente, A.M., Rocha, S., Vasconcellos, P., 2017. Hopanoid hydrocarbons in PM_{10} from road tunnels in São Paulo, Brazil. Air Qual. Atmos. Health. 10, 799-807.

Alves, C.A., Vicente, A.M.P., Gomes, J., Nunes, T., Duarte, M., Bandowe, B.A.M. 2016. Polycyclic aromatic hydrocarbons (PAHs) and their derivatives (oxygenated-PAHs, nitrated-PAHs and azaarenes) in size-fractionated particles emitted in an urban road tunnel. Atmos. Res. 180, 128-137.

Amato, F., Alastuey, A., Karanasiou, A., Lucarelli, F., Nava, S., Calzolai, G., Severi, M., Becagli, S., Gianelle, V.L., Colombi, C., Alves, C., Custódio, D., Nunes, T., Cerqueira, M., Pio, C., Eleftheriadis, K., Diapouli, E., Reche, C., Minguillón, M.C., Manousakas, M.I., Maggos, T., Vratolis, S., Harrison, R.M., Querol X., 2016. AIRUSE-LIFE+: a harmonized PM speciation and source apportionment in five southern European cities. Atmos. Chem. Phys. 16, 3289-3309.

Amato, F., 2018. Non-Exhaust Emissions. An Urban Air Quality Problem for Public Health; Impact and Mitigation Measures. 1st Edition. Academic Press, United Kingdom.

Amato, F., Cassee, F.R., Denier van der Gon, H.A., Gehrig, R., Gustafsson, M., Hafner, W., Harrison, R.M., Jozwicka, M. Kelly, F.J., Moreno, T., Prevot, A.S., Schaap, M., Sunyer, J., Querol X., 2014. Urban air quality: The challenge of traffic non-exhaust emissions. J. Hazard. Mater. 275, 31-36.

Attademo, L., Bernardini, F., 2017. Air pollution and urbanicity: common risk factors for dementia and schizophrenia? Lancet Planet. Health 1, e90-e91.

Babadjouni, R.M., Hodis, D.M., Radwanski, R., Durazo, R., Patel, A., Liu, Q., Mack, W.J., 2017. Clinical effects of air pollution on the central nervous system: a review. J. Clin. Neurosci. 43, 16-24.

Block, M.L., Elder, A., Auten, R.L., Bilbo, S.D., Chen, H., Chen, J.C., Cory-Slechta, D.A., Costa, D., Diaz-Sanchez, D., Dorman, D.C., Gold, D.R., Gray, K., Jeng, H.A., Kaufman, J.D., Kleinman, M.T., Kirshner, A., Lawler, C., Miller, D.S., Nadadur, S.S., Ritz, B., Semmens, E.O., Tonelli, L.H., Veronesi, B., Wright, R.O, Wright, R.J., 2012. The outdoor air pollution and brain health workshop. Neurotoxicology 33, 972-984.

Boonyatumanond, R., Murakami, M., Wattayakorn, G., Togo, A., Takada, H., 2007. Sources of polycyclic aromatic hydrocarbons (PAHs) in street dust in a tropical Asian mega-city, Bangkok, Thailand. Sci. Total Environ. 384, 420-432.

Boulter, P.G., 2006. A review of emission factors and models for road vehicle non-exhaust particulate matter. TRL Report PPR065. TRL Limited, Wokingham.

Brunekreef, B., Forsberg, B., 2005. Epidemiological evidence of effects of coarse airborne particles on health. Eur. Respir. J. 26, 309-318.

Cadle S.H., Williams, R.L., 1979. Gas and particle emissions from automobile tires in laboratory and field studies. Rubber Chem. Technol. 52, 146-158.

Calvo, A.I., Alves, C., Castro, A., Pont, V., Vicente, A.M., Fraile, R., 2013. Research on aerosol sources and chemical composition: past, current and emerging issues. Atmos. Res. 120-121, 1-28.

Chang, Y., Liu, X., Dore, A.J., Li, K., 2012. Stemming $PM_{2.5}$ pollution in China: Re-evaluating the role of ammonia, aviation and non-exhaust road traffic emissions. Environ. Sci. Technol. 46, 13035-13036.

Chen, H., Kwong, J.C., Copes, R., Tu, K., Villeneuve, P.R., van Donkelaar, A., Hystad, P., Martin, R.V., Murray, B.J., Jessiman, B., Wilton, A.S., Kopp, A., Burnett, R.T., 2017. Living near major roads and the incidence of dementia, Parkinson's disease, and multiple sclerosis: a population-based cohort study. Lancet 389, 718-726.

Councell, T.B., Duckenfield, K.U., Landa, E.R., Callender, E., 2004. Tire-wear particles as a source of zinc to the environment. Environ. Sci. Technol. 38, 4206-4214.

Dahl, A., Gharibi, A., Swietlicki, E., Gudmundsson, A., Bohgard, M., Ljungman, A., Blomqvist, G., Gustafsson, M., 2006. Traffic-generated emissions of ultrafine particles from pavement-tire interface. Atmos. Environ. 40, 1314-1323.

Dall'Osto, M., Beddows, D.C.S., Gietl, J.K., Olatunbosun, O.A., Yang, X., Harrison, R.M., 2014. Characteristics of tyre dust in polluted air: Studies by single particle mass spectrometry (ATOFMS). Atmos. Environ. 94 224-230.

Downard, J., Singh, A., Bullard, R., Jayarathne, T., Rathnayake, C.M., Simmons, D.L., Wels, B.R., Spak, S.N., Peters, T., Beardsley, D., Stanier, C.O., Stone, E.A., 2015. Uncontrolled combustion of shredded tires in a landfill e Part 1: Characterization of gaseous and particulate emissions. Atmos. Environ. 104, 195-204.

Foitzik, M.J., Unrau, H.J., Gauterin, F., Dörnhöfer, J., Koch, T., 2018. Investigation of ultra-fine particulate matter emission of rubber tires. Wear, 394-395, 87-95.

Formela, K., Wasowicz, D., Formela, M., Hejna, A., Haponiuk, J., 2015. Curing characteristics, mechanical and thermal properties of reclaimed ground tire rubber cured with various vulcanizing systems. Iran. Polym. J. 24, 289-297.

Fry, C., Jarvis, K.E., Parry, S.J., 2008. Diagnostic tool for source apportionment of heavy metals around roads. Science report SC000030. Environment Agency, Bristol, UK.

Gadd, J., P. Kennedy, 2003. Preliminary examination of organic compounds present in tyres, brake pads, and road bitumen in New Zealand. Prepared by Kingett Mitchell Limited for Ministry of Transport (Te Manatū Waka). New Zealand.

Gao, Q., Xu, Q., Guo, X., Fan, H., Zhu, H., 2017. Particulate matter air pollution associated with hospital admissions for mental disorders: a time-series study in Beijing, China. Eur. Psychiatry. 44, 68-75.

Gonçalves, C., Alves, C., Fernandes, A.P., Monteiro, C., Tarelho, L., Evtyugina, M., Pio C, 2011. Organic compounds in $PM_{2.5}$ emitted from fireplace and woodstove combustion of typical Portuguese wood species. Atmos. Environ. 45, 4533-4545.

Grigoratos, T., Gustafsson, M., Eriksson, O., Martini, G., 2018. Experimental investigation of tread wear and particle emission from tyres with different treadwear marking. Atmos. Environ. 182, 200-212.

Grigoratos, T., Martini, G., 2014. Non-Exhaust Traffic Related Emissions. Brake and Tyre Wear PM. Literature Survey. JRC Science and Policy Reports 2014. Luxembourg: Publications Office of the European Union. 10.2790/21481

Gualtieri, M., Mantecca, P., Cetta, F., Camatini, M., 2008. Organic compounds in tire particle induce reactive oxygen species and heat-shock proteins in the human alveolar cell line A549. Environ. Int. 34, 437-442.

Gustafsson, M., Blomqvist, G., Gudmundsson, A., Dahl, A., Jonsson, P., Swietlicki, E., 2009. Factors influencing PM_{10} emissions from road pavement wear. Atmos. Environ. 43 4699-4702.

Gustafsson, M., Blomqvist, G., Gudmundsson, A., Dahl, A., Swietlicki, E., Bohgard, M., Lindbom, J., Ljungman, A., 2008. Properties and toxicological effects of particles from the interaction between tyres, road pavement and winter traction material. Sci. Total Environ. 393, 226-240.

Haghighat, M., Khorasani, S.N., Zadhoush, A., 2007. Filler-rubber interactions in α_cellulose-filled styrene butadiene rubber composites. Polym. Composite. 28, 748-754.

Harrison, R.M., Jones, A.M., Gietl, J., Yin, J., Green, D.C., 2012. Estimation of the contributions of brake dust, tire wear, and resuspension to non-exhaust traffic particles derived from atmospheric measurements. Environ. Sci. Technol. 46, 6523-6529.

Health Effects Institute, 2017. State of Global Air 2017. Special Report. Boston, MA.

Hjortenkrans, D.S.T., Bergback, B.G., Haggerud, A.V., 2007. Metal emissions from brake linings and tires: case studies of Stockholm, Sweden 1995/1998 and 2005. Environ. Sci. Technol. 41, 5224-5230

Hosiokangas, J., Vallius, M., Ruuskanen, J., Mirme, A., Pekkanen, J., 2004. Resuspended dust episodes as an urban air-quality problem in subarctic regions. Scand. J. Work Environ. Health 30, 28-35.

International Agency for Research on Cancer, 2016. IARC Monographs on the Evaluation of Carcinogenic Risks to Humans. Vol. 109, Outdoor Air Pollution. Lyon, France.

Karagulian, F., Belis, C.A., Dora, C.F.C., Prüss-Ustün, A.M., Bonjour, S., Adair-Rohani, H., Amann, M., 2015. Contributions to cities' ambient particulate matter (PM): A systematic review of local source contributions at global level. Atmos. Environ. 120, 475-483.

Kim, G., Lee, S., 2018. Characteristics of tire wear particles generated by a tire simulator. Environ. Sci. Technol. Environ. Sci. Technol. 52, 12153-12161.

Kole, P.J., Löhr, A.J., Van Belleghem, F.G.A.J., Ragas, A.M.J., 2017. Wear and tear of tyres: A stealthy source of microplastics in the environment. Int. J. Environ. Res. Public Health 14, 1265. doi: 10.3390/ijerph14101265

Kreider, M.L., Panko, J.M., McAtee, B.L., Sweet, L.I., Finley, B.L., 2010. Physical and chemical characterization of tire-related particles: Comparison of particles generated using different methodologies. Sci. Total Environ. 408, 652-659.

Kumar, P., Morawska, L., Birmili, W., Paasonen, P., Hu, M., Kulmala, M., Harrison, R. M., Norford, L., Britter, R., 2014. Ultrafine particles in cities. Environ. Int., 66, 1–10.

Kumata, H., Mori, M., Takahashi, S., Takamiya, S., Tsuzuki, M., Uchida, T., Fujiwara, K., 2011. Evaluation of hydrogenated resin acids as molecular markers for tire-wear debris in urban environments. Environ. Sci. Technol. 45, 9990-9997.

Kupiainen, K.J., Tervahattu, H., Raisanen, M., Makela, T., Aurela, M., Hillamo, R., 2005. Size and composition of airborne particles from pavement wear, tires, and traction sanding. Environ. Sci. Technol. 39, 699-706.

Kwon, E.E., Castaldi, M.J., 2012. Mechanistic understanding of polycyclic aromatic hydrocarbons (PAHs) from the thermal degradation of tires under various oxygen concentration atmospheres. Sci. Total Environ. 46, 12921-12926.

Lawton, K., Cherrier, V., Grebot, B., Zglobisz, N., Esparrago, J., Ganzleben, C., Kallay, T., Farmer, A., 2014. Study on: "Contribution of industry to pollutant emissions to air and water". Final Report. AMEC Environment & Infrastructure UK Limited in partnership with Bio Intelligence Service, Milieu, IEEP and REC. European Commission (DG Environment). Publications Office of the European Union, Luxembourg.

Lee, B.J., Kim, B., Lee. K., 2014. Air pollution exposure and cardiovascular disease. Toxicol. Res. 30, 71-75.

Lee, S., Kwak, J., Kim, H., Lee, J., 2013. Properties of roadway particles from interaction between the tire and road pavement. Int. J. Automot. Technol. 14,163-173.

Lee, K.K., Miller, M.R., Shah, A.S.V., 2018. Air pollution and stroke. J. Stroke 20, 2-11.

Lelieveld, J., Evans, J.S., Fnais, M., Giannadaki, D., Pozzer, A., 2015. The contribution of outdoor air pollution sources to premature mortality on a global scale. Nature 525, 367-371.

Lelieveld, J., Klingmüller, K., Pozzer, A., Pöschl, U., Fnaism M., Daiber, A., Münzel, T., 2019. Cardiovascular disease burden from ambient air pollution in Europe reassessed using novel hazard ratio functions. Eur. Heart J. 40, 1590-1596.

Llompart, M., Sanchez-Prado, L., Lamas, J.P., Garcia-Jares, C., Roca, E., Dagnac, T., 2013. Hazardous organic chemicals in rubber recycled tire playgrounds and pavers. Chemosphere 90, 423-43.

Loomis, D., Grosse, Y., Lauby-Secretan, B., El Ghissassi. F., Bouvard, V., Benbrahim-Tallaa, L., Guha, N., Baan, R., Mattock, H., Straif, K., 2014. IARC evaluation of the carcinogenicity of outdoor air pollution. Environ. Risque Sante 13, 347-352.

Luhana L. Sokhi R., Warner L., Mao H., Boulter P., McCrae I., Wright J., Osborn D., 2004. Deliverable 8 from 5th Framework Programme Project “PARTICULATES”, European Commision, Directorate General Transport and Environment.

Marwood, C., McAtee, B., Kreider, M., Ogle, R.S., Finley, B., Sweet, .L, Panko, J., 2011. Acute aquatic toxicity of tire and road wear particles to alga, daphnid, and fish. Ecotoxicol. 20, 2079-2089.

Mathissen, M., Scheer, V., Vogt, R., Benter, T., 2011. Investigation on the potential generation of ultrafine particles from the tire-road interface. Atmos. Environ. 45, 6172-6179.

Meister, K., Johansson, C., Forsberg, B., 2012. Estimated short-term effects of coarse particles on daily mortality in Stockholm, Sweden. Environ. Health Perspect. 120, 431-436.

Newby, D.E., Mannucci, P.M., Tell, G.S., Baccarelli, A.A., Brook, R.D., Donaldson. K., Forastiere, F., Franchini, M., Franco, O.H., Graham, I., Hoek, G., Hoffmann, B., Hoylaerts, M.F., Künzli, N., Mills, N., Pekkanen, J., Peters, A., Piepoli, MF., Rajagopalan, S., Storey, R.F., ESC Working Group on Thrombosis, European Association for Cardiovascular Prevention and Rehabilitation, ESC Heart Failure

Association, 2015. Expert position paper on air pollution and cardiovascular disease. Eur. Heart J. 36, 83-93.

Nolte, C.G., Schauer, J.J., Cass, G.R., Simoneit, B.R.T., 2002. Trimethylsilyl derivatives of organic compounds in source samples and in atmospheric fine particulate matter. Environ. Sci. Technol. 36, 4273-4281.

Padoan, E., Amato, F., 2018. Vehicle Non-Exhaust Emissions: Impact on Air Quality. In: Non-Exhaust Emissions. An Urban Air Quality Problem for Public Health; Impact and Mitigation Measures. Amato, F. (Editor), Chapter 2, Academic Press, London. 21-65, https://doi.org/10.1016/B978-0-12-811770-5.00002-9

Panko, J.M., Chu, J., Kreider, M., Unice, K.M., 2013b. Measurement of airborne concentrations of tire and road wear particles in urban and rural areas of France, Japan, and the United States. Atmos. Environ. 72, 192-199.

Panko, J.M., Kreider, M.L., McAtee, B.L., Marwood, C., 2013a. Chronic toxicity of tire and road wear particles to water- and sediment-dwelling organisms. Ecotoxicol. 22, 13-21.

Pant, P., Harrison, R.M., 2013. Estimation of the contribution of road traffic emissions to particulate matter concentrations from field measurements: A review. Atmos. Environ. 77, 78-97.

Pant, P., Shi, Z., Pope, F.D., Harrison, R.M., 2017. Characterization of traffic-related particulate matter emissions in a road tunnel in Birmingham, UK: Trace metals and organic molecular markers. Aerosol Air Qual. Res. 17, 117-130.

Park, I., Lee, J., Lee, S., 2017. Laboratory study of the generation of nanoparticles from tire tread. Aerosol Sci. Technol. 51, 188-197.

Perez, L., Medina, M., Künzli, N., Alastuey, A., Pey, J., Perez, N., Garcia, R., Tobias, A., Querol, X., Sunyer, J., 2009. Size fractionate particulate matter, vehicular traffic, and case-specific daily mortality in Barcelona (Spain). Environ. Sci. Technol. 43, 4707-4714.

Pio, C., Cerqueira, M., Harrison, R.M., Nunes, T., Mirante, F., Alves, C., Oliveira, C., Sanchez de la Campa, A., Artiñano, B., Matos, M., 2011. OC/EC Ratio Observations in Europe: Re-thinking the approach for apportionment between primary and secondary organic carbon. Atmos. Environ. 45, 6121-6132.

Querol, X., Alastuey, A., Rodriguez, S., Plana, F., Ruiz, C.R., Cots, N., Massagué, G., Puig, O., 2001. PM_{10} and $PM_{2.5}$ source apportionment in the Barcelona Metropolitan Area, Catalonia, Spain. Atmos. Environ. 35, 6407-6419.

Querol, X., Alastuey, A., Ruiz, C.R., Artiñano, B., Hansson, H.C., Harrison, R.M., Buringh, E., ten Brink. H.M., Lutz, M., Bruckmann, P., 2004. Speciation and origin of PM_{10} and $PM_{2.5}$ in selected European cities. Atmos. Environ. 38, 6547-6555.

Ramdahl, T., 1983. Retene - a molecular marker of wood combustion in ambient air. Nature 306, 580-582.

Rogge, W.F., Hildemann, L.M., Mazurek, M.A., Cass, G.R., Simoneit, B.R.T., 1993. Sources of fine organic aerosol. 3. Road dust, tire debris, and organometallic brake lining dust: roads as sources and sinks. Environ. Sci. Technol. 27, 1892-1904.

Sadiktsis, I., Bergvall, C., Johansson, C., Westerholm, R., 2012. Automobile tires - A potential source of highly carcinogenic dibenzopyrenes to the environment. Environ. Sci. Technol. 46, 3326-3334.

Shah, A.S.V., Lee, K.K., McAllister, D.A., Hunter, A., Nair, H., Whiteley, W., Langrish,J.P., Newby,D.E., Mills, N.L., 2015. Short term exposure to air pollution and stroke: systematic review and meta-analysis. BMJ 350. https://doi.org/10.1136/bmj.h1295

Sjödin, A., Ferm, M., Björk, A., Rahmberg, M., Gudmundsson, A., Swietlicki, E., Johansson, C., Gustafsson, M. Blomqvist, G., 2010. Wear particles from road traffic: A field, laboratory and modelling study. IVL Swedish Environmental Research Institute Ltd., Göteborg.

Sram, R.J., Veleminsky, M.Jr, Veleminsky, M.Sr., Stejskalová, J., 2017. The impact of air pollution to central nervous system in children and adults. Neuro Endocrinol. Lett. 38, 389-396.

Swietlicki, E., Nilsson., T., Kristensson, A., Johansson, C., Omstedt, G., Gidhagen, L., 2004. Traffic-related source contributions to PM_{10} near a highway. J. Aerosol Sci. 35, S795-S796.

Thorpe, A., Harrison, R.M., 2008. Sources and properties of non-exhaust particulate matter from road traffic: A review. Sci. Total Environ. 400, 270-282.

Uherek, E., Halenka, T., Borken-Kleefeld, J., Balkanski, Y., Berntsen, T., Borrego, C., Gauss, M., Hoor, P., Juda-Rezler, K., Lelieveld, J., Melas, D., Rypdal, K., Schmid, S., 2010. Transport impacts on atmosphere and climate: Land transport. Atmos. Environ. 44, 4772–4816.

van der Gon, H.A., Gerlofs-Nijland, M.E., Gehrig, R., Gustafsson, M., Janssen, N., Harrison, R.M., Hulskotte, J., Johansson, C., Jozwicka, M., Keuken, M., Krijgsheld, K., Ntziachristos, L., Riediker, M., Cassee, F.R., 2013. The policy relevance of wear emissions from road transport, now and in the future--an international workshop report and consensus statement. J. Air Waste Manag. Assoc. 63, 136-149.

Vicente, E.D., Alves, C.A., 2018. An overview of particulate emissions from residential biomass combustion. Atmos. Res. 199, 159-185.

Wagner, S., Hüffer, T., Klöckner, P., Wehrhahn, M., Hofmann, T., Reemtsma, T., 2018. Tire wear particles in the aquatic environment - A review on generation, analysis, occurrence, fate and effects. Water Res. 139, 83-100.

Wik A., Dave G., 2009. Occurrence and effects of tire wear particles in the environment - a critical review and an initial risk assessment. Environ. Pollut. 157, 1-11.

Zmozinski, A.V., de Jesus, A., Vale, M.G., Silva, M.M., 2010. Determination of calcium, magnesium and zinc in lubricating oils by flame atomic absorption spectrometry using a three-component solution. Talanta 83, 637-643.

SUPPLEMENTARY MATERIAL

Comparison between APS and TEOM

The average values for the three runs (see Fig. 1), when both instruments were being operated, are compared to one another in Figure S1. The higher values obtained from the TEOM are likely a result of mass measured by this instrument related to particles smaller than the lower size threshold of the APS.

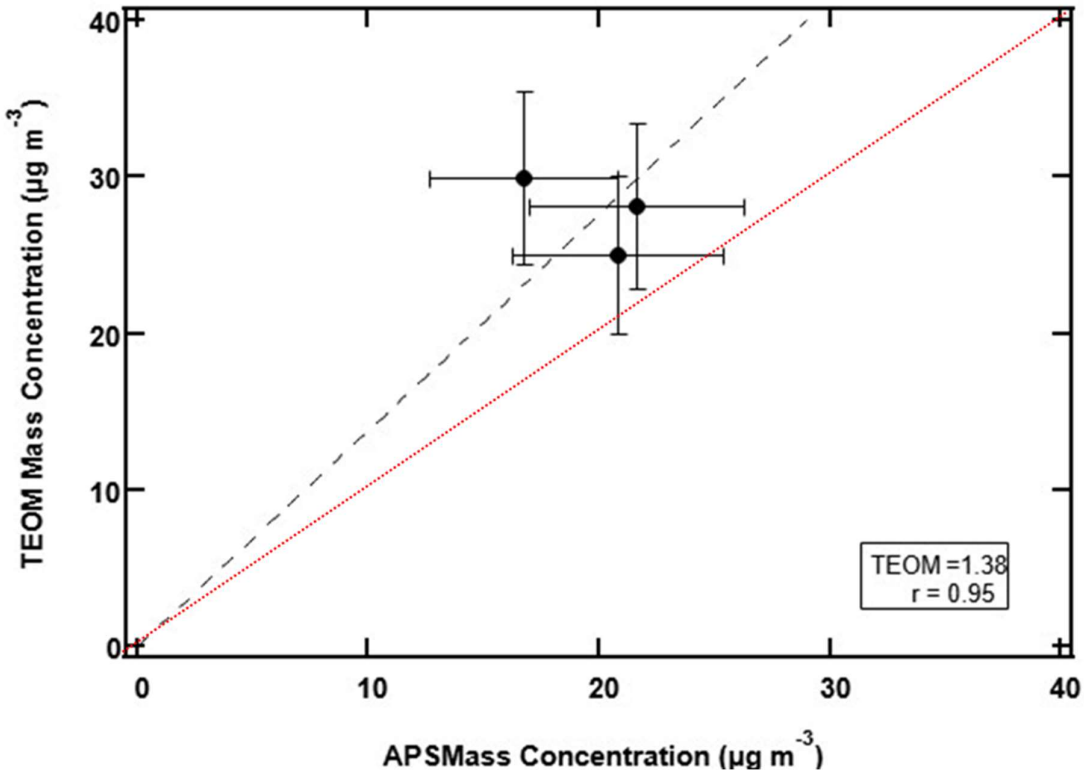

Figure S1. Comparison between mass concentration measurements from the TEOM and APS.

Estimation of emissions factors

The emission rate Q is derived from the fit to the equation

$$M(t)=M_0\, e^{-Kt} + (Q/K)(1- e^{-Kt})$$

that was originally developed from a box model that assumed that the particle production was balanced by particle sedimentation. The emission factor, EF, is derived by considering the volume of the chamber where the tests were taking place and the velocity of the tyres. If the tyres are producing particles at a mass emission rate of m µg per second and the velocity is v km s^{-1}, then the emission rate per kilometer is m/v. If the volume of the measurement chamber is V cm^3, and the measured mass concentration of M µg m^{-3}, then the total mass in the chamber, M_{total}, that is being produced by the tyres is MV. Assuming that once the sedimentation rate balances the production rate, then the EF (mg km^{-1}) can be derived.

PM_{10} mass balance

To obtain a PM_{10} mass balance (Fig. S2), the measured element concentrations were converted into the respective mass concentrations of the most common oxides (Al_2O_3, CaO, MgO, MnO, Fe_2O_3, TiO_2, K_2O, etc.). Because the GC-MS analyses indicated the presence of highly oxygenated compounds, to derive the organic matter content in PM_{10}, a total organic mass to organic carbon ratio (OM/OC) of 2.0 was adopted (Polidori et al., 2008). In addition to sampling and analysis artefacts affecting the attainment of chemical mass balance, the unaccounted mass can partly be explained by the presence of unanalysed constituents. Furthermore, part of the unaccounted PM_{10} mass is usually assigned to particle-bound water (Tsyro, 2005).

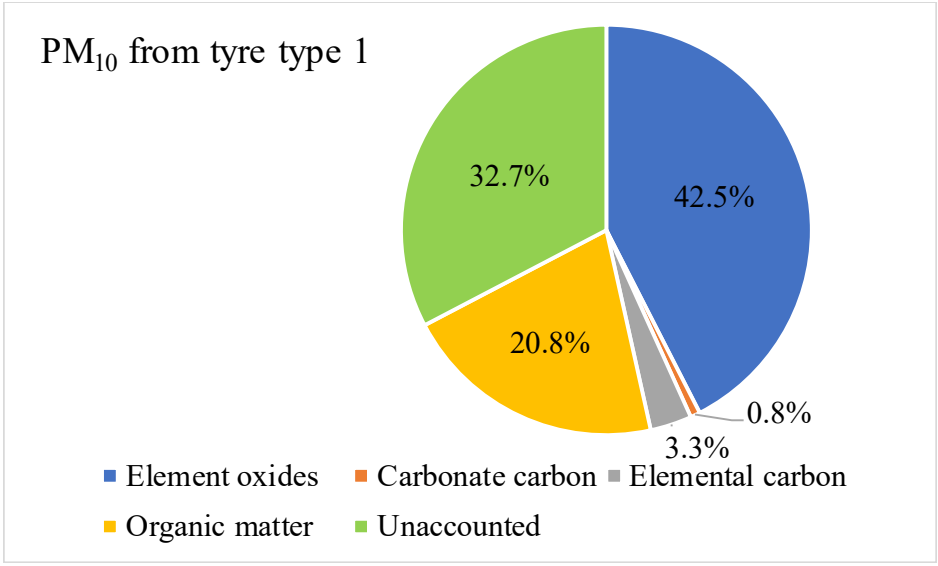

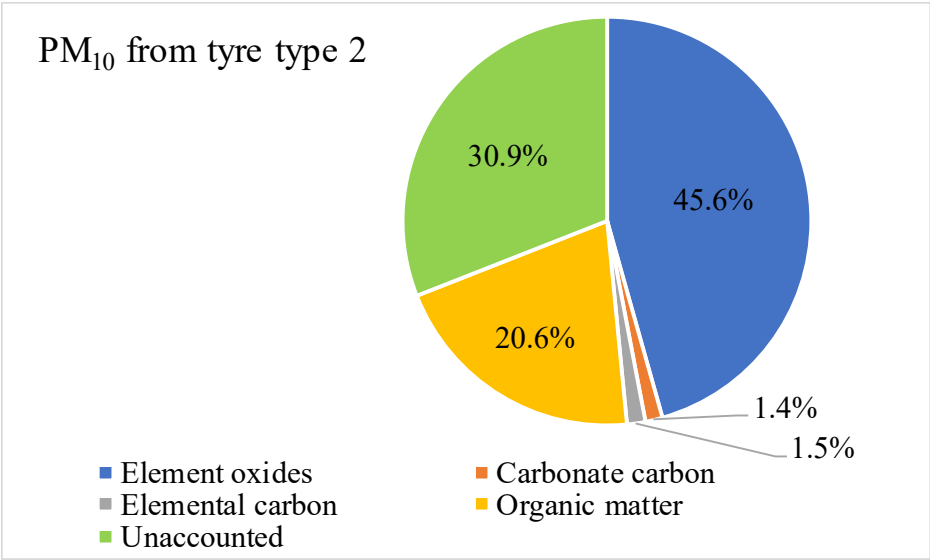

Figure S2. Chemical mass balance of PM_{10} from tyre-pavement wear.

Organic composition

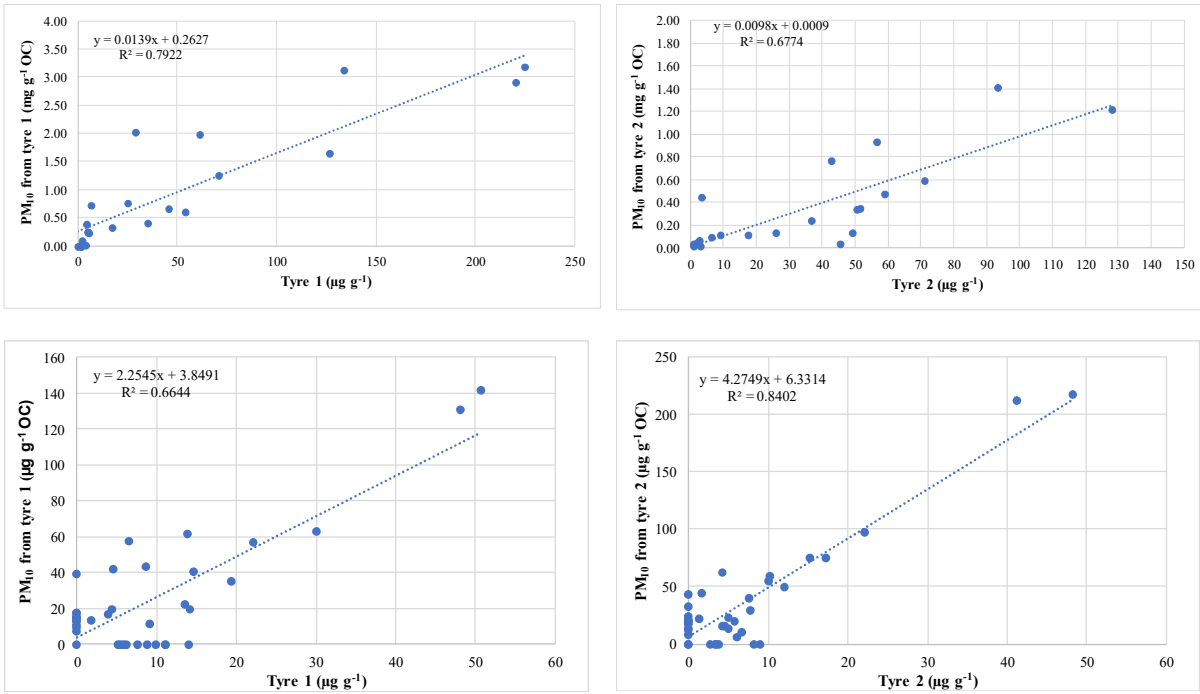

Figure S3. Correlations between the mass concentrations in tyres and the OC-normalised concentrations in PM_{10}. Upper panels: *n*-alkanes from C_{12} to C_{30}; Lower panels: hopanoid and triterpenoid compounds.

Table S1. Organic compounds detected in PM_{10} from tyre wear and in tyre tread

	PM_{10} from tyre type 1 (µg g^{-1})	PM_{10} from tyre type 2 (µg g^{-1})	Tyre type 1 (µg g^{-1})	Tyre type 2 (µg g^{-1})
***n*-Alkanols**				
1-Decanol	0.583	2.03	0.020	-
1-Pentadecanol	-	-	0.130	22.9
1-Hexadecanol	15,945	17,324	-	2.13
1-Octadecanol	-	5750	-	-
1-Docosanol	48.0	20.9	0.325	0.108
1-Tricosanol	39.8	22.8	0.862	0.954
1-Pentacosanol	36.5	20.8	0.596	0.801
1-Heptacosanol	19.0	13.5	-	-
1-Octacosanol	58.4	66.7	1.60	-
1-Triacontanol	17.1	15.5	-	-
***n*-Alkanoic acids**				
Octanoic acid	-	124	0.610	1.76
Nonanoic acid	176	464	1.26	2.71
Decanoic acid	111	265	-	4.43
Undecanoic acid	125	193	0.259	0.683
Dodecanoic acid	1,268	1,309	3.98	9.97
Tridecanoic acid	141	87.2	0.317	0.567
Tetradecanoic acid	904	830	45.2	201
Pentadecanoic acid	131	47.7	11.0	12.6
Hexadecanoic acid	5654	7,789	285	1,281
Heptadecanoic acid	46.3	-	52.0	119

Octadecanoic acid	8,284	9428	589	1,464
Nonadecanoic acid	25.4	7.40	3.13	3.75
Eicosanoic acid	1,566	-	137	231
Docosanoic acid	260	77.0	1.67	2.31
Tetracosanoic acid	176	-	-	-
Di- and tricarboxylic acids				
Citric acid	4.10	-	-	-
Ethanedioic acid	179	98.6	-	-
Malonic acid	87.4	29.6	0.468	0.812
Malic acid	193	-	0.777	-
Succinic acid	256	-	-	0.657
Pentanedioic acid	225	7.38	-	0.593
Hexanedioic acid	50.0	-	-	0.580
Heptanedioic acid	170	131	0.067	0.219
Octanedioic acid	65.9	-	0.276	0.606
Nonanedioic acid	177	-	1.33	2.69
Decanedioic acid	24.8	-	0.058	0.142
Hydroxy- and oxo-acids				
Pentanoic acid, 4-oxo-	25.6	34.9	0.00	0.00
Glycolic acid	1026	1198	8.82	20.8
3-Hydroxybutyric acid	119	91.7	0.209	0.322
D-Gluconic acid	21.0	0.00	0.058	0.090
Unsaturated fatty acids				
Palmitoleic acid	0.00	0.00	0.00	64.4
Linoleic acid	13.6	0.00	3.41	2.47
Oleic Acid	47.0	0.00	147	1360
Resin acids				
Pinic acid	709	174	0.00	0.271
Isopimaric Acid	0.00	0.00	0.00	11.5
Dehydroabietic acid	463	441	248	2142
Abietic acid	82.5	0.00	0.00	9.06
Aromatic acids				
Benzoic acid	205	311	1.90	13.4
Cinnamic acid	60.3	-	0.058	0.064
Hydrocinnamic acid	-	-	0.418	0.422
4-Hydroxybenzoic acid	28.2	4.48	0.050	0.142
2,3,4-Trimethoxybenzoic acid	-	-	-	0.232
p-Coumaric acid	3.17	1.23	-	-
Ferulic acid	0.710	-	-	-
Phthalic acid	64.6	-	-	-
Phthalates				
Diisobutyl phthalate	2,265	43,818	-	-
Dibutyl phthalate	25,474	37,085	3.71	4.05
Dicyclohexyl phthalate	-	-	-	33.2
Isooctyl phthalate	16,507	28,228	-	-
Bis(2-ethylhexyl) phthalate	3.90	267	0.442	2.50
Diethyl phthalate	-	-	0.158	0.240
Acid esters				
Phosphoric acid tributyl ester	936	0.00	0.00	0.00
Hexanedioic acid, bis(2-methylpropyl) ester	243	304	0.00	0.00
Phthalic acid, octyl propyl ester	0.00	1080	0.00	0.00
Hexanedioic acid, dioctyl ester	963	1902	0.00	0.00
Phosphoric acid, 2-ethylhexyl diphenyl ester	0.00	109	0.00	0.00
Monoterpenes				
Myrtenol	15.58	1.64	0.357	0.431
β-Citronellol	0.672	-	0.0073	-
Verbenol	48.3	-	-	-
2,3-Pinanediol	101	-	0.138	0.106
Isopulegol	7.30	1.94	0.126	0.122
Polyols				
Xylitol	484	183	0.262	0.268
Meso-Erythritol	2.86	8.01	-	-
D-Sorbitol	1,306	1,018	0.464	0.769

Quebrachitol	50.8	-	-	-
1-Monolauroyl-rac-Glycerol	3.04	6.85	0.774	1.07
Ribitol	215	73.1	-	-
Saccharides				
Galactosan	180	-	-	-
Mannosan	691	132	-	-
Levoglucosan	3,217	427	0.893	0.949
Mannose	278	208	-	0.913
Ribose	118	-	-	-
Glucose	350	241	0.405	1.32
Sucrose	86.4	58.2	-	-
Maltose monohydrate	850	351	-	-
Sucrose	176	191	-	-
Cyclic alcohols				
Methylcyclohexanol	-	-	-	0.545
Cyclohexanol	42.5	27.3	-	1.64
Benzyl alcohol	640	5,499	216	368
Sterols and triterpenoids				
Cholesterol	89.4	62.3	0.549	1.09
Stigmasterol	11.2	11.6	1.07	0.664
β-Sitosterol	30.3	16.4	8.36	5.35
Lupeol	12.8	6.08	0.039	-
Urs-12-en-3-one	0.862	0.850	0.085	0.014
Lupenone	2.24	10.68	0.137	-
Phenolics				
4-Octylphenol	137	-	-	-
Vanillin	0.121	0.525	0.023	0.028
Vanillic acid	28.4	0.212	0.092	-
Syringic acid	7.85	-	-	-
Syringaldehyde	0.355	0.858	0.001	0.001
Sinapinaldehyde	140	220	0.547	0.300
Acetosyringone	4.75	7.24	-	8.05
Lactones				
D-Glucuronic acid lactone	141	88.7	0.000	0.438
γ-Undecalactone	8.69	47.3	0.075	0.066
Coumarin	8.03	12.8	0.012	0.018
Other ketones				
Tridecan-2-one	1.34	9.38	0.017	0.011
Hexadecan-3-one	95.3	100	0.359	1.17
Octadecan-2-one	174	256	-	-
Fluoren-9-one	36.3	50.9	0.326	0.449
2,6-di-tert-Butyl-p-benzoquinone	-	119	-	-
Acetylacetophenone	82.2	-	-	-
7,9-Di-tert-butyl-1-oxaspiro(4,5)deca-6,9-diene-2,8-dione	538	-	0.615	1.17
Diacetone alcohol	-	29.3	-	2.38
N- and S- containing compounds				
Hexamethyldisilathiane	-	-	13.2	9.95
Isocyanatocyclohexane	-	23.8	2.89	-
Cyclohexanamine	-	-	8.04	-
2,4-Dimethylquinoline	638	538	-	-
Diphenylcarbodiimide	-	-	9.74	3.86
Benzenamine	-	-	2.18	-
N,N-Dibutyl-1-butanamine	91.3	126	1.20	-
Phenylisocyanate	-	-	6.76	-
5-Hydroxyindole-2-carboxylic acid	-	-	3.17	20.1
Dibenzothiophene (DBT)	2.41	2.22	0.196	0.670

858 **References**

859

860 Polidori, A., Turpin, B.J., Davidson, C.I., Rodenburg, L.A., Maimone, F., 2008. Organic $PM_{2.5}$: fractionation
861 by polarity, FTIR spectroscopy, and OM/OC ratio for the Pittsburgh aerosol. Aerosol Sci. Technol. 42,
862 233-246

863 Tsyro, S.G., 2005. To what extent can aerosol water explain the discrepancy between model calculated and
864 gravimetric PM_{10} and $PM_{2.5}$? Atmos. Chem. Phys. 5, 515-532.